Target Atmospheric CO_2: Where Should Humanity Aim?

James Hansen[*,1,2], Makiko Sato[1,2], Pushker Kharecha[1,2], David Beerling[3], Robert Berner[4], Valerie Masson-Delmotte[5], Mark Pagani[4], Maureen Raymo[6], Dana L. Royer[7] and James C. Zachos[8]

[1]*NASA/Goddard Institute for Space Studies, New York, NY 10025, USA*

[2]*Columbia University Earth Institute, New York, NY 10027, USA*

[3]*Department of Animal and Plant Sciences, University of Sheffield, Sheffield S10 2TN, UK*

[4]*Department of Geology and Geophysics, Yale University, New Haven, CT 06520-8109, USA*

[5]*Lab. Des Sciences du Climat et l'Environnement/Institut Pierre Simon Laplace, CEA-CNRS-Universite de Versailles Saint-Quentin en Yvelines, CE Saclay, 91191, Gif-sur-Yvette, France*

[6]*Department of Earth Sciences, Boston University, Boston, MA 02215, USA*

[7]*Department of Earth and Environmental Sciences, Wesleyan University, Middletown, CT 06459-0139, USA*

[8]*Earth & Planetary Sciences Dept., University of California, Santa Cruz, Santa Cruz, CA 95064, USA*

Abstract: Paleoclimate data show that climate sensitivity is ~3°C for doubled CO_2, including only fast feedback processes. Equilibrium sensitivity, including slower surface albedo feedbacks, is ~6°C for doubled CO_2 for the range of climate states between glacial conditions and ice-free Antarctica. Decreasing CO_2 was the main cause of a cooling trend that began 50 million years ago, the planet being nearly ice-free until CO_2 fell to 450 ± 100 ppm; barring prompt policy changes, that critical level will be passed, in the opposite direction, within decades. If humanity wishes to preserve a planet similar to that on which civilization developed and to which life on Earth is adapted, paleoclimate evidence and ongoing climate change suggest that CO_2 will need to be reduced from its current 385 ppm to at most 350 ppm, but likely less than that. The largest uncertainty in the target arises from possible changes of non-CO_2 forcings. An initial 350 ppm CO_2 target may be achievable by phasing out coal use except where CO_2 is captured and adopting agricultural and forestry practices that sequester carbon. If the present overshoot of this target CO_2 is not brief, there is a possibility of seeding irreversible catastrophic effects.

Keywords: Climate change, climate sensitivity, global warming.

1. INTRODUCTION

Human activities are altering Earth's atmospheric composition. Concern about global warming due to long-lived human-made greenhouse gases (GHGs) led to the United Nations Framework Convention on Climate Change [1] with the objective of stabilizing GHGs in the atmosphere at a level preventing "dangerous anthropogenic interference with the climate system."

The Intergovernmental Panel on Climate Change [IPCC, [2]] and others [3] used several "reasons for concern" to estimate that global warming of more than 2-3°C may be dangerous. The European Union adopted 2°C above pre-industrial global temperature as a goal to limit human-made warming [4]. Hansen *et al.* [5] argued for a limit of 1°C global warming (relative to 2000, 1.7°C relative to pre-industrial time), aiming to avoid practically irreversible ice sheet and species loss. This 1°C limit, with nominal climate sensitivity of ¾°C per W/m^2 and plausible control of other GHGs [6], implies maximum CO_2 ~ 450 ppm [5].

Our current analysis suggests that humanity must aim for an even lower level of GHGs. Paleoclimate data and ongoing global changes indicate that 'slow' climate feedback processes not included in most climate models, such as ice sheet disintegration, vegetation migration, and GHG release from soils, tundra or ocean sediments, may begin to come into play on time scales as short as centuries or less [7]. Rapid on-going climate changes and realization that Earth is out of energy balance, implying that more warming is 'in the pipeline' [8], add urgency to investigation of the dangerous level of GHGs.

A probabilistic analysis [9] concluded that the long-term CO_2 limit is in the range 300-500 ppm for 25 percent risk tolerance, depending on climate sensitivity and non-CO_2 forcings. Stabilizing atmospheric CO_2 and climate requires that net CO_2 emissions approach zero, because of the long lifetime of CO_2 [10, 11].

*Address correspondence to this author at the NASA/Goddard Institute for Space Studies, New York, NY 10025, USA; E-mail: jhansen@giss.nasa.gov

1874-2823/08

We use paleoclimate data to show that long-term climate has high sensitivity to climate forcings and that the present global mean CO_2, 385 ppm, is already in the dangerous zone. Despite rapid current CO_2 growth, ~2 ppm/year, we show that it is conceivable to reduce CO_2 this century to less than the current amount, but only *via* prompt policy changes.

1.1. Climate Sensitivity

A global climate forcing, measured in W/m^2 averaged over the planet, is an imposed perturbation of the planet's energy balance. Increase of solar irradiance (So) by 2% and doubling of atmospheric CO_2 are each forcings of about 4 W/m^2 [12].

Charney [13] defined an idealized climate sensitivity problem, asking how much global surface temperature would increase if atmospheric CO_2 were instantly doubled, assuming that slowly-changing planetary surface conditions, such as ice sheets and forest cover, were fixed. Long-lived GHGs, except for the specified CO_2 change, were also fixed, not responding to climate change. The Charney problem thus provides a measure of climate sensitivity including only the effect of 'fast' feedback processes, such as changes of water vapor, clouds and sea ice.

Classification of climate change mechanisms into fast and slow feedbacks is useful, even though time scales of these changes may overlap. We include as fast feedbacks aerosol changes, e.g., of desert dust and marine dimethylsulfide, that occur in response to climate change [7].

Charney [13] used climate models to estimate fast-feedback doubled CO_2 sensitivity of 3 ± 1.5°C. Water vapor increase and sea ice decrease in response to global warming were both found to be strong positive feedbacks, amplifying the surface temperature response. Climate models in the current IPCC [2] assessment still agree with Charney's estimate.

Climate models alone are unable to define climate sensitivity more precisely, because it is difficult to prove that models realistically incorporate all feedback processes. The Earth's history, however, allows empirical inference of both fast feedback climate sensitivity and long-term sensitivity to specified GHG change including the slow ice sheet feedback.

2. PLEISTOCENE EPOCH

Atmospheric composition and surface properties in the late Pleistocene are known well enough for accurate assessment of the fast-feedback (Charney) climate sensitivity. We first compare the pre-industrial Holocene with the last glacial maximum [LGM, 20 ky BP (before present)]. The planet was in energy balance in both periods within a small fraction of 1 W/m^2, as shown by considering the contrary: an imbalance of 1 W/m^2 maintained a few millennia would melt all ice on the planet or change ocean temperature an amount far outside measured variations [Table **S1** of 8]. The approximate equilibrium characterizing most of Earth's history is unlike the current situation, in which GHGs are rising at a rate much faster than the coupled climate system can respond.

Climate forcing in the LGM equilibrium state due to the ice age surface properties, i.e., increased ice area, different vegetation distribution, and continental shelf exposure, was -3.5 ± 1 W/m^2 [14] relative to the Holocene. Additional forcing due to reduced amounts of long-lived GHGs (CO_2, CH_4, N_2O), including the indirect effects of CH_4 on tropospheric ozone and stratospheric water vapor (Fig. **S1**) was -3 ± 0.5 W/m^2. Global forcing due to slight changes in the Earth's orbit is a negligible fraction of 1 W/m^2 (Fig. **S3**). The total 6.5 W/m^2 forcing and global surface temperature change of 5 ± 1°C relative to the Holocene [15, 16] yield an empirical sensitivity ~¾ ± ¼ °C per W/m^2 forcing, i.e., a Charney sensitivity of 3 ± 1 °C for the 4 W/m^2 forcing of doubled CO_2. This empirical fast-feedback climate sensitivity allows water vapor, clouds, aerosols, sea ice, and all other fast feedbacks that exist in the real world to respond naturally to global climate change.

Climate sensitivity varies as Earth becomes warmer or cooler. Toward colder extremes, as the area of sea ice grows, the planet approaches runaway snowball-Earth conditions, and at high temperatures it can approach a runaway greenhouse effect [12]. At its present temperature Earth is on a flat portion of its fast-feedback climate sensitivity curve (Fig. **S2**). Thus our empirical sensitivity, although strictly the mean fast-feedback sensitivity for climate states ranging from the ice age to the current interglacial period, is also today's fast-feedback climate sensitivity.

2.1. Verification

Our empirical fast-feedback climate sensitivity, derived by comparing conditions at two points in time, can be checked over the longer period of ice core data. Fig. (**1a**) shows CO_2 and CH_4 data from the Antarctic Vostok ice core [17, 18] and sea level based on Red Sea sediment cores [18]. Gases are from the same ice core and have a consistent time scale, but dating with respect to sea level may have errors up to several thousand years.

We use the GHG and sea level data to calculate climate forcing by GHGs and surface albedo change as in prior calculations [7], but with two refinements. First, we specify the N_2O climate forcing as 12 percent of the sum of the CO_2 and CH_4 forcings, rather than the 15 percent estimated earlier [7] Because N_2O data are not available for the entire record, and its forcing is small and highly correlated with CO_2 and CH_4, we take the GHG effective forcing as

$$\text{Fe (GHGs)} = 1.12\,[\text{Fa}(CO_2) + 1.4\,\text{Fa}(CH_4)], \quad (1)$$

using published formulae for Fa of each gas [20]. The factor 1.4 accounts for the higher efficacy of CH_4 relative to CO_2, which is due mainly to the indirect effect of CH_4 on tropospheric ozone and stratospheric water vapor [12]. The resulting GHG forcing between the LGM and late Holocene is 3 W/m^2, apportioned as 75% CO_2, 14% CH_4 and 11% N_2O.

The second refinement in our calculations is to surface albedo. Based on models of ice sheet shape, we take the horizontal area of the ice sheet as proportional to the 4/5 power of volume. Fig. (**S4**) compares our present albedo forcing with prior use [7] of exponent 2/3, showing that this

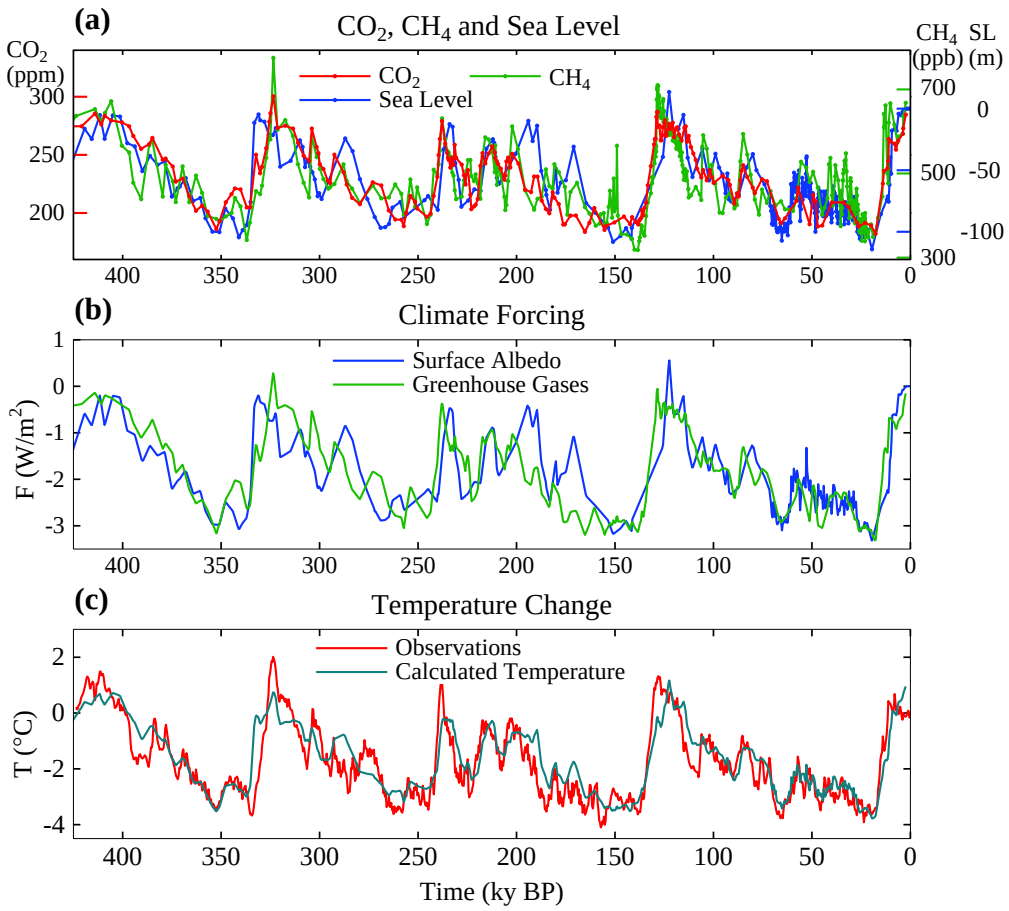

Fig. (1). (**a**) CO_2, CH_4 [17] and sea level [19] for past 425 ky. (**b**) Climate forcings due to changes of GHGs and ice sheet area, the latter inferred from sea level change. (**c**) Calculated global temperature change based on climate sensitivity of ¾°C per W/m^2. Observations are Antarctic temperature change [18] divided by two.

choice and division of the ice into multiple ice sheets has only a minor effect.

Multiplying the sum of GHG and surface albedo forcings by climate sensitivity ¾°C per W/m^2 yields the blue curve in Fig. (**1c**). Vostok temperature change [17] divided by two (red curve) is used to crudely estimate global temperature change, as typical glacial-interglacial global annual-mean temperature change is ~5°C and is associated with ~10°C change on Antarctica [21]. Fig. (**1c**) shows that fast-feedback climate sensitivity ¾°C per W/m^2 (3°C for doubled CO_2) is a good approximation for the entire period.

2.2. Slow Feedbacks

Let us consider climate change averaged over a few thousand years – long enough to assure energy balance and minimize effects of ocean thermal response time and climate change leads/lags between hemispheres [22]. At such temporal resolution the temperature variations in Fig. (**1**) are global, with high latitude amplification, being present in polar ice cores and sea surface temperature derived from ocean sediment cores (Fig. **S5**).

GHG and surface albedo changes are mechanisms causing the large global climate changes in Fig. (**1**), but they do not initiate these climate swings. Instead changes of GHGs and sea level (a measure of ice sheet size) lag temperature change by several hundred years [6, 7, 23, 24].

GHG and surface albedo changes are positive climate feedbacks. Major glacial-interglacial climate swings are instigated by slow changes of Earth's orbit, especially the tilt of Earth's spin-axis relative to the orbital plane and the precession of the equinoxes that influences the intensity of summer insolation [25, 26]. Global radiative forcing due to orbital changes is small, but ice sheet size is affected by changes of geographical and seasonal insolation (e.g., ice melts at both poles when the spin-axis tilt increases, and ice melts at one pole when perihelion, the closest approach to the sun, occurs in late spring [7]. Also a warming climate causes net release of GHGs. The most effective GHG feedback is release of CO_2 by the ocean, due partly to temperature dependence of CO_2 solubility but mostly to increased ocean mixing in a warmer climate, which acts to flush out

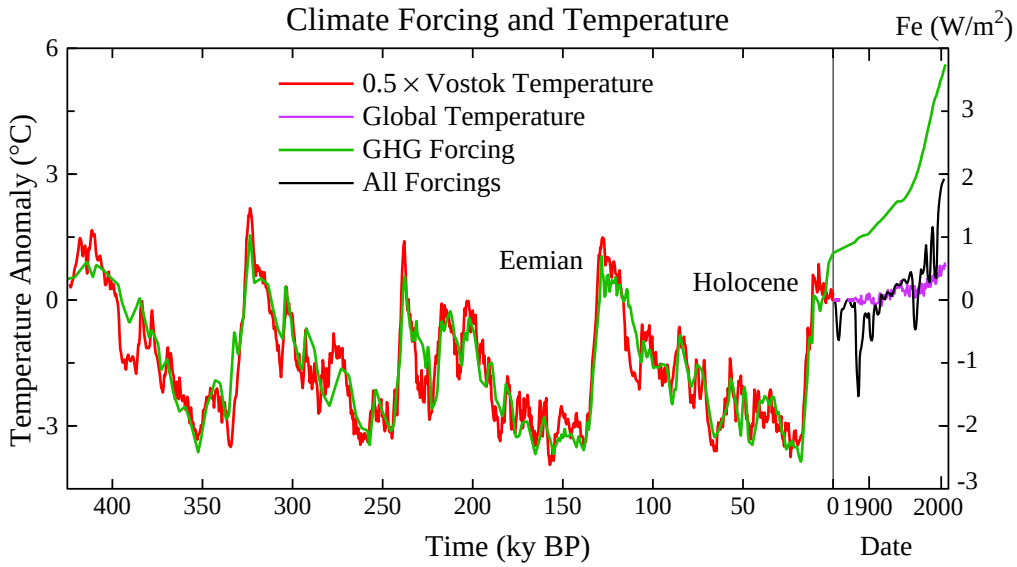

Fig. (2). Global temperature (left scale) and GHG forcing (right scale) due to CO_2, CH_4 and N_2O from the Vostok ice core [17, 18]. Time scale is expanded for the industrial era. Ratio of temperature and forcing scales is 1.5°C per W/m^2, i.e., the temperature scale gives the expected equilibrium response to GHG change including (slow feedback) surface albedo change. Modern forcings include human-made aerosols, volcanic aerosols and solar irradiance [5]. GHG forcing zero point is the mean for 10-8 ky BP (Fig. **S6**). Zero point of modern temperature and net climate forcing was set at 1850 [5], but this is also the zero point for 10-8 ky BP, as shown by the absence of a trend in Fig. (**S6**) and by the discussion of that figure.

deep ocean CO_2 and alters ocean biological productivity [27].

GHG and surface albedo feedbacks respond and contribute to temperature change caused by any climate forcing, natural or human-made, given sufficient time. The GHG feedback is nearly linear in global temperature during the late Pleistocene (Fig. **7** of [6, 28]). Surface albedo feedback increases as Earth becomes colder and the area of ice increases. Climate sensitivity on

Pleistocene time scales includes slow feedbacks, and is larger than the Charney sensitivity, because the dominant slow feedbacks are positive. Other feedbacks, e.g., the negative feedback of increased weathering as CO_2 increases, become important on longer geologic time scales.

Paleoclimate data permit evaluation of long-term sensitivity to specified GHG change. We assume only that, to first order, the area of ice is a function of global temperature. Plotting GHG forcing [7] from ice core data [18] against temperature shows that global climate sensitivity including the slow surface albedo feedback is 1.5°C per W/m^2 or 6°C for doubled CO_2 (Fig. **2**), twice as large as the Charney fast-feedback sensitivity. Note that we assume the area of ice and snow on the planet to be predominately dependent on global temperature, but some changes of regional ice sheet properties occur as part of the Earth orbital climate forcing (see Supplementary Material).

This equilibrium sensitivity of 6°C for doubled CO_2 is valid for specified GHG amount, as in studies that employ emission scenarios and coupled carbon cycle/climate models to determine GHG amount. If GHGs are included as a feedback (with say solar irradiance as forcing) sensitivity is still larger on Pleistocene time scales (see Supplementary Material), but the sensitivity may be reduced by negative feedbacks on geologic time scales [29, 30]. The 6°C sensitivity reduces to 3°C when the planet has become warm enough to lose its ice sheets.

This long-term climate sensitivity is relevant to GHGs that remain airborne for centuries-to-millennia. The human-caused atmospheric GHG increase will decline slowly if anthropogenic emissions from fossil fuel burning decrease enough, as we illustrate below using a simplified carbon cycle model. On the other hand, if the globe warms much further, carbon cycle models [2] and empirical data [6, 28] reveal a positive GHG feedback on century-millennia time scales. This amplification of GHG amount is moderate if warming is kept within the range of recent interglacial periods [6], but larger warming would risk greater release of CH_4 and CO_2 from methane hydrates in tundra and ocean sediments [29]. On still longer, geological, time scales weathering of rocks causes a negative feedback on atmospheric CO_2 amount [30], as discussed in section 3, but this feedback is too slow to alleviate climate change of concern to humanity.

2.3. Time Scales

How long does it take to reach equilibrium temperature with specified GHG change? Response is slowed by ocean thermal inertia and the time needed for ice sheets to disintegrate.

Ocean-caused delay is estimated in Fig. (**S7**) using a coupled atmosphere-ocean model. One-third of the response occurs in the first few years, in part because of rapid response over land, one-half in ~25 years, three-quarters in 250 years, and nearly full response in a millennium. The ocean-

caused delay is a strong (quadratic) function of climate sensitivity and it depends on the rate of mixing of surface water and deep water [31], as discussed in the Supplementary Material Section.

Ice sheet response time is often assumed to be several millennia, based on the broad sweep of paleo sea level change (Fig. **1a**) and primitive ice sheet models designed to capture that change. However, this long time scale may reflect the slowly changing orbital forcing, rather than inherent inertia, as there is no discernable lag between maximum ice sheet melt rate and local insolation that favors melt [7]. Paleo sea level data with high time resolution reveal frequent 'suborbital' sea level changes at rates of 1 m/century or more [32-34].

Present-day observations of Greenland and Antarctica show increasing surface melt [35], loss of buttressing ice shelves [36], accelerating ice streams [37], and increasing overall mass loss [38]. These rapid changes do not occur in existing ice sheet models, which are missing critical physics of ice sheet disintegration [39]. Sea level changes of several meters per century occur in the paleoclimate record [32, 33], in response to forcings slower and weaker than the present human-made forcing. It seems likely that large ice sheet response will occur within centuries, if human-made forcings continue to increase. Once ice sheet disintegration is underway, decadal changes of sea level may be substantial.

2.4. Warming "in the Pipeline"

The expanded time scale for the industrial era (Fig. **2**) reveals a growing gap between actual global temperature (purple curve) and equilibrium (long-term) temperature response based on the net estimated climate forcing (black curve). Ocean and ice sheet response times together account for this gap, which is now 2.0°C.

The forcing in Fig. (**2**) (black curve, Fe scale), when used to drive a global climate model [5], yields global temperature change that agrees closely (Fig. **3** in [5]) with observations (purple curve, Fig. **2**). That climate model, which includes only fast feedbacks, has additional warming of ~0.6°C in the pipeline today because of ocean thermal inertia [5, 8].

The remaining gap between equilibrium temperature for current atmospheric composition and actual global temperature is ~1.4°C. This further 1.4°C warming still to come is due to the slow surface albedo feedback, specifically ice sheet disintegration and vegetation change.

One may ask whether the climate system, as the Earth warms from its present 'interglacial' state, still has the capacity to supply slow feedbacks that double the fast-feedback sensitivity. This issue can be addressed by considering longer time scales including periods with no ice.

3. CENOZOIC ERA

Pleistocene atmospheric CO_2 variations occur as a climate feedback, as carbon is exchanged among surface reservoirs: the ocean, atmosphere, soils and biosphere. The most effective feedback is increase of atmospheric CO_2 as climate warms, the CO_2 transfer being mainly from ocean to atmosphere [27, 28]. On longer time scales the total amount of CO_2 in the surface reservoirs varies due to exchange of carbon with the solid earth. CO_2 thus becomes a primary agent of long-term climate change, leaving orbital effects as 'noise' on larger climate swings.

The Cenozoic era, the past 65.5 My, provides a valuable complement to the Pleistocene for exploring climate sensitivity. Cenozoic data on climate and atmospheric composition are not as precise, but larger climate variations occur, including an ice-free planet, thus putting glacial-interglacial changes in a wider perspective.

Oxygen isotopic composition of benthic (deep ocean dwelling) foraminifera shells in a global compilation of ocean sediment cores [26] provides a starting point for analyzing Cenozoic climate change (Fig. **3a**). At times with negligible ice sheets, oxygen isotope change, $\delta^{18}O$, provides a direct measure of deep ocean temperature (T_{do}). Thus T_{do} (°C) ~ -4 $\delta^{18}O$ + 12 between 65.5 and 35 My BP.

Rapid increase of $\delta^{18}O$ at about 34 My is associated with glaciation of Antarctica [26, 40] and global cooling, as evidenced by data from North America [41] and Asia [42]. From then until the present, ^{18}O in deep ocean foraminifera is affected by both ice volume and T_{do}, lighter ^{16}O evaporating preferentially from the ocean and accumulating in ice sheets. Between 35 My and the last ice age (20 ky) the change of $\delta^{18}O$ was ~ 3‰, change of T_{do} was ~ 6°C (from +5 to -1°C) and ice volume change ~ 180 msl (meters of sea level). Given that a 1.5‰ change of $\delta^{18}O$ is associated with a 6°C T_{do} change, we assign the remaining $\delta^{18}O$ change to ice volume linearly at the rate 60 msl per mil $\delta^{18}O$ change (thus 180 msl for $\delta^{18}O$ between 1.75 and 4.75). Equal division of $\delta^{18}O$ between temperature and sea level yields sea level change in the late Pleistocene in reasonable accord with available sea level data (Fig. **S8**). Subtracting the ice volume portion of $\delta^{18}O$ yields deep ocean temperature T_{do} (°C) = -2 ($\delta^{18}O$ -4.25‰) after 35 My, as in Fig. (**3b**).

The large (~14°C) Cenozoic temperature change between 50 My and the ice age at 20 ky must have been forced by changes of atmospheric composition. Alternative drives could come from outside (solar irradiance) or the Earth's surface (continental locations). But solar brightness increased ~0.4% in the Cenozoic [43], a linear forcing change of only +1 W/m^2 and of the wrong sign to contribute to the cooling trend. Climate forcing due to continental locations was < 1 W/m^2, because continents 65 My ago were already close to present latitudes (Fig. **S9**). Opening or closing of oceanic gateways might affect the timing of glaciation, but it would not provide the climate forcing needed for global cooling.

CO_2 concentration, in contrast, varied from ~180 ppm in glacial times to 1500 ± 500 ppm in the early Cenozoic [44]. This change is a forcing of more than 10 W/m^2 (Table **1** in [16]), an order of magnitude larger than other known forcings. CH_4 and N_2O, positively correlated with CO_2 and global temperature in the period with accurate data (ice cores), likely increase the total GHG forcing, but their forcings are much smaller than that of CO_2 [45, 46].

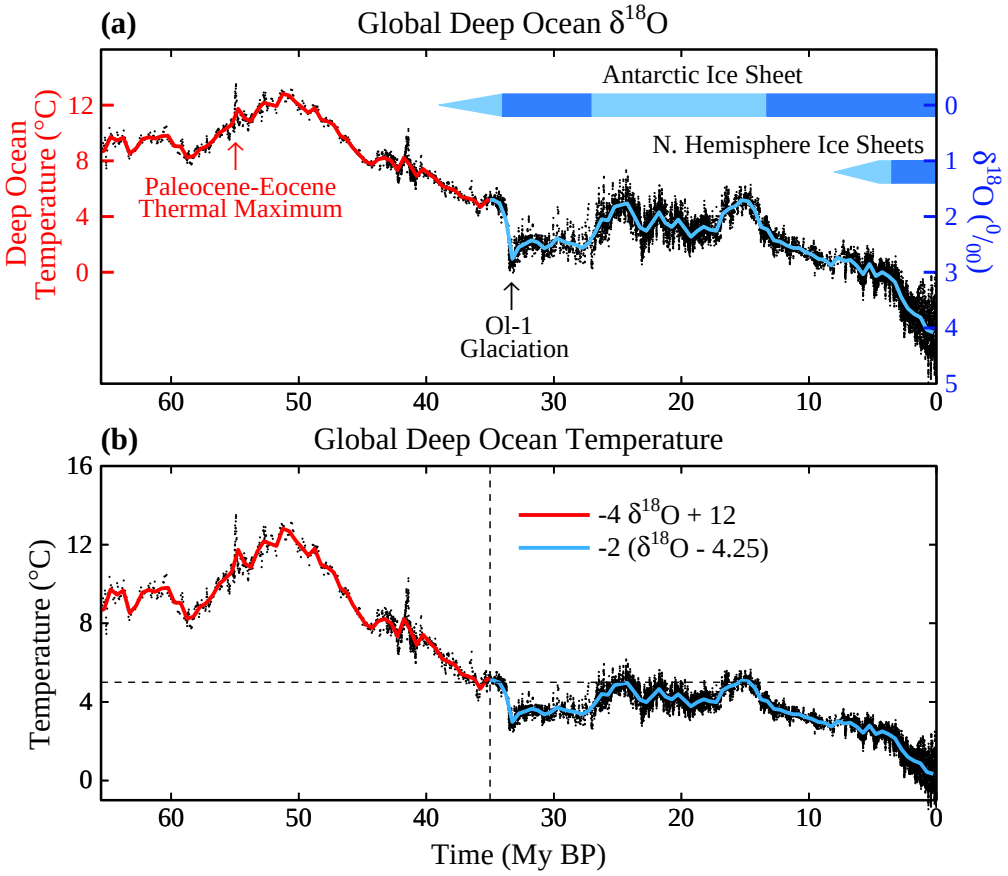

Fig. (3). Global deep ocean (**a**) $\delta^{18}O$ [26] and (**b**) temperature. Black curve is 5-point running mean of $\delta^{18}O$ original temporal resolution, while red and blue curves have 500 ky resolution.

3.1. Cenozoic Carbon Cycle

Solid Earth sources and sinks of CO_2 are not, in general, balanced at any given time [30, 47]. CO_2 is removed from surface reservoirs by: (1) chemical weathering of rocks with deposition of carbonates on the ocean floor, and (2) burial of organic matter; weathering is the dominant process [30]. CO_2 returns primarily *via* metamorphism and volcanic outgassing at locations where carbonate-rich oceanic crust is being subducted beneath moving continental plates.

Outgassing and burial of CO_2 are each typically 10^{12}-10^{13} mol C/year [30, 47-48]. At times of unusual plate tectonic activity, such as rapid subduction of carbon-rich ocean crust or strong orogeny, the imbalance between outgassing and burial can be a significant fraction of the one-way carbon flux. Although negative feedbacks in the geochemical carbon cycle reduce the rate of surface reservoir perturbation [49], a net imbalance ~10^{12} mol C/year can be maintained over thousands of years. Such an imbalance, if confined to the atmosphere, would be ~0.005 ppm/year, but as CO_2 is distributed among surface reservoirs, this is only ~0.0001 ppm/year. This rate is negligible compared to the present human-made atmospheric CO_2 increase of ~2 ppm/year, yet over a million years such a crustal imbalance alters atmospheric CO_2 by 100 ppm.

Between 60 and 50 My ago India moved north rapidly, 18-20 cm/year [50], through a region that long had been a depocenter for carbonate and organic sediments. Subduction of carbon-rich crust was surely a large source of CO_2 outgassing and a prime cause of global warming, which peaked 50 My ago (Fig. **3b**) with the Indo-Asian collision. CO_2 must have then decreased due to a reduced subduction source and enhanced weathering with uplift of the Himalayas/Tibetan Plateau [51]. Since then, the Indian and Atlantic Oceans have been major depocenters for carbon, but subduction of carbon-rich crust has been limited mainly to small regions near Indonesia and Central America [47].

Thus atmospheric CO_2 declined following the Indo-Asian collision [44] and climate cooled (Fig. **3b**) leading to Antarctic glaciation by ~34 My. Antarctica has been more or less glaciated ever since. The rate of CO_2 drawdown declines as atmospheric CO_2 decreases due to negative feedbacks, including the effect of declining atmospheric temperature and plant growth rates on weathering [30]. These negative feedbacks tend to create a balance between crustal outgassing and drawdown of CO_2, which have been equal within 1-2 percent over the past 700 ky [52]. Large fluctuations in the size of the Antarctic ice sheet have occurred in the past 34 My, possibly related to temporal variations of plate tectonics [53] and outgassing rates. The relatively constant atmos-

pheric CO_2 amount of the past 20 My (Fig. **S10**) implies a near balance of outgassing and weathering rates over that period.

Knowledge of Cenozoic CO_2 is limited to imprecise proxy measures except for recent ice core data. There are discrepancies among different proxy measures, and even between different investigators using the same proxy method, as discussed in conjunction with Fig. (**S10**). Nevertheless, the proxy data indicate that CO_2 was of the order of 1000 ppm in the early Cenozoic but <500 ppm in the last 20 My [2, 44].

3.2. Cenozoic Forcing and CO_2

The entire Cenozoic climate forcing history (Fig. **4a**) is implied by the temperature reconstruction (Fig. **3b**), assuming a fast-feedback sensitivity of ¾°C per W/m^2. Subtracting the solar and surface albedo forcings (Fig. **4b**), the latter from Eq. S2 with ice sheet area *vs* time from $\delta^{18}O$, we obtain the GHG forcing history (Fig. **4c**).

We hinge our calculations at 35 My for several reasons. Between 65 and 35 My ago there was little ice on the planet, so climate sensitivity is defined mainly by fast feedbacks. Second, we want to estimate the CO_2 amount that precipitated Antarctic glaciation. Finally, the relation between global surface air temperature change (ΔT_s) and deep ocean temperature change (ΔT_{do}) differs for ice-free and glaciated worlds.

Climate models show that global temperature change is tied closely to ocean temperature change [54]. Deep ocean temperature is a function of high latitude ocean surface temperature, which tends to be amplified relative to global mean ocean surface temperature. However, land temperature change exceeds that of the ocean, with an effect on global temperature that tends to offset the latitudinal variation of ocean temperature. Thus in the ice-free world (65-35 My) we take $\Delta T_s \sim \Delta T_{do}$ with generous (50%) uncertainty. In the glaciated world ΔT_{do} is limited by the freezing point in the deep ocean. ΔT_s between the last ice age (20 ky) and the present

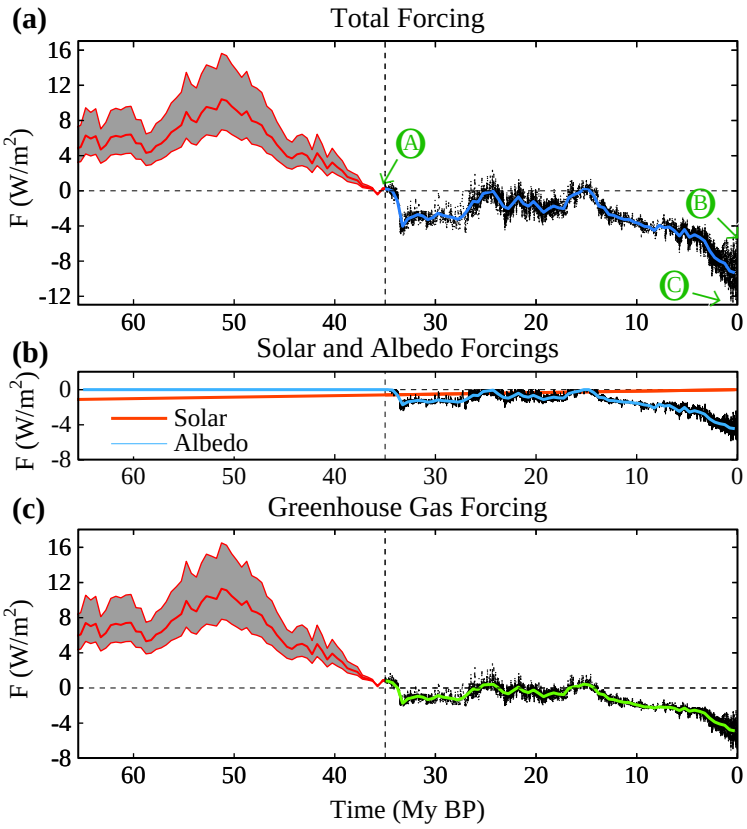

Fig. (4). (**a**) Total climate forcing, (**b**) solar and surface albedo forcings, and (**c**) GHG forcing in the Cenozoic, based on T_{do} history of Fig. (**3b**) and assumed fast-feedback climate sensitivity ¾°C per W/m^2. Ratio of T_s change and T_{do} change is assumed to be near unity in the minimal ice world between 65 and 35 My, but the gray area allows for 50% uncertainty in the ratio. In the later era with large ice sheets we take $\Delta T_s/\Delta T_{do} = 1.5$, in accord with Pleistocene data.

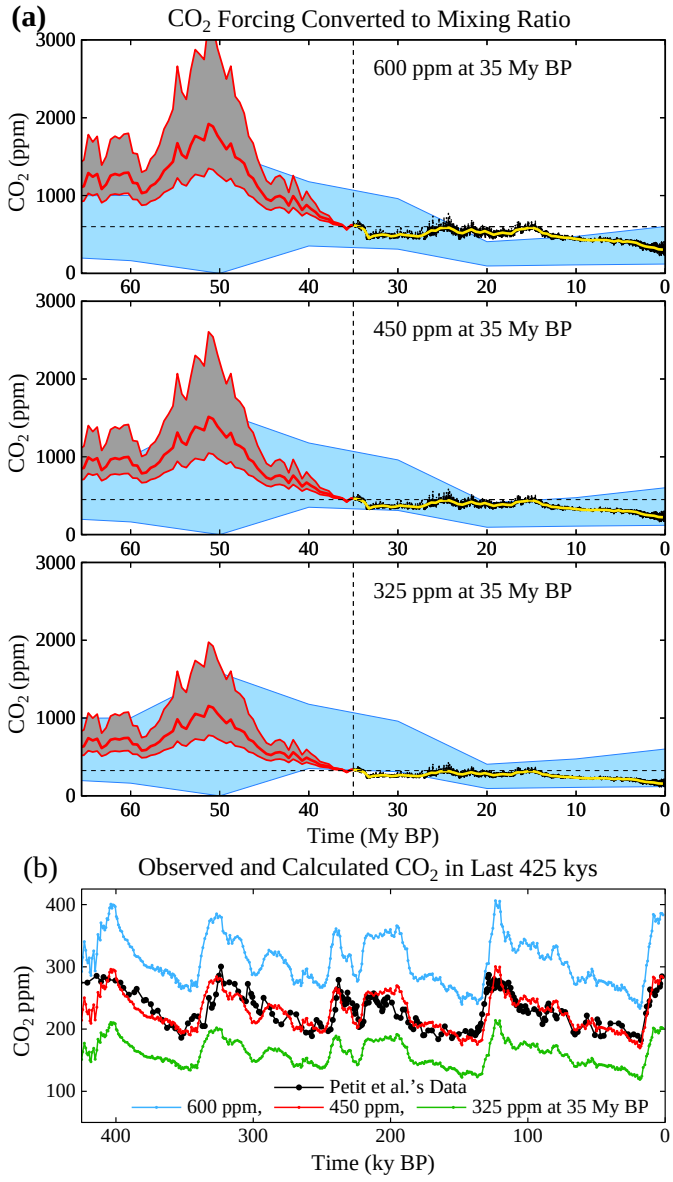

Fig. (5). (**a**) Simulated CO_2 amounts in the Cenozoic for three choices of CO_2 amount at 35 My (temporal resolution of black and colored curves as in Fig. (**3**); blue region: multiple CO_2 proxy data, discussed with Fig. (**S10**); gray region allows 50 percent uncertainty in ratio of global surface and deep ocean temperatures). (**b**) Expanded view of late Pleistocene, including precise ice core CO_2 measurements (black curve).

interglacial period (~5°C) was ~1.5 times larger than ΔT_{do}. In Fig. (**S5**) we show that this relationship fits well throughout the period of ice core data.

If we specify CO_2 at 35 My, the GHG forcing defines CO_2 at other times, assuming CO_2 provides 75% of the GHG forcing, as in the late Pleistocene. CO_2 ~450 ppm at 35 My keeps CO_2 in the range of early Cenozoic proxies (Fig. **5a**) and yields a good fit to the amplitude and mean CO_2 amount in the late Pleistocene (Fig. **5b**). A CO_2 threshold for Antarctic glaciation of ~500 ppm was previously inferred from proxy CO_2 data and a carbon cycle model [55].

Individual CO_2 proxies (Fig. **S10**) clarify limitations due to scatter among the measurements. Low CO_2 of some early Cenozoic proxies, if valid, would suggest higher climate

sensitivity. However, in general the sensitivities inferred from the Cenozoic and Phanerozoic [56, 57, 58] agree well with our analysis, if we account for the ways in which sensitivity is defined and the periods emphasized in each empirical derivation (Table **S1**).

Our CO_2 estimate of ~450 ppm at 35 My (Fig. **5**) serves as a prediction to compare with new data on CO_2 amount. Model uncertainties (Fig. **S10**) include possible changes of non-CO_2 GHGs and the relation of ΔT_s to ΔT_{do}. The model fails to account for cooling in the past 15 My if CO_2 increased, as several proxies suggest (Fig. **S10**). Changing ocean currents, such as the closing of the Isthmus of Panama, may have contributed to climate evolution, but models find little effect on temperature [59]. Non-CO_2 GHGs also could have played a role, because little forcing would have been needed to cause cooling due to the magnitude of late Cenozoic albedo feedback.

3.3. Implication

We infer from Cenozoic data that CO_2 was the dominant Cenozoic forcing, that CO_2 was ~450 ± 100 ppm when Antarctica glaciated, and that glaciation is reversible. Together these inferences have profound implications.

Consider three points marked in Fig. (**4**): point A at 35 My, just before Antarctica glaciated; point B at recent interglacial periods; point C at the depth of recent ice ages. Point B is about half way between A and C in global temperature (Fig. **3b**) and climate forcings (Fig. **4**). The GHG forcing from the deepest recent ice age to current interglacial warmth is ~3.5 W/m^2. Additional 4 W/m^2 forcing carries the planet, at equilibrium, to the ice-free state. Thus equilibrium climate sensitivity to GHG change, including the surface albedo change as a slow feedback, is almost as large between today and an ice-free world as between today and the ice ages.

The implication is that global climate sensitivity of 3°C for doubled CO_2, although valid for the idealized Charney definition of climate sensitivity, is a considerable understatement of expected equilibrium global warming in response to imposed doubled CO_2. Additional warming, due to slow climate feedbacks including loss of ice and spread of flora over the vast high-latitude land area in the Northern Hemisphere, approximately doubles equilibrium climate sensitivity.

Equilibrium sensitivity 6°C for doubled CO_2 is relevant to the case in which GHG changes are specified. That is appropriate to the anthropogenic case, provided the GHG amounts are estimated from carbon cycle models including climate feedbacks such as methane release from tundra and ocean sediments. The equilibrium sensitivity is even higher if the GHG feedback is included as part of the climate response, as is appropriate for analysis of the climate response to Earth orbital perturbations. The very high sensitivity with both albedo and GHG slow feedbacks included accounts for the huge magnitude of glacial-interglacial fluctuations in the Pleistocene (Fig. **3**) in response to small forcings (section 3 of Supplementary Material).

Equilibrium climate response would not be reached in decades or even in a century, because surface warming is slowed by the inertia of the ocean (Fig. **S7**) and ice sheets. However, Earth's history suggests that positive feedbacks, especially surface albedo changes, can spur rapid global warmings, including sea level rise as fast as several meters per century [7]. Thus if humans push the climate system sufficiently far into disequilibrium, positive climate feedbacks may set in motion dramatic climate change and climate impacts that cannot be controlled.

4. ANTHROPOCENE ERA

Human-made global climate forcings now prevail over natural forcings (Fig. **2**). Earth may have entered the Anthropocene era [60, 61] 6-8 ky ago [62], but the net human-made forcing was small, perhaps slightly negative [7], prior to the industrial era. GHG forcing overwhelmed natural and negative human-made forcings only in the past quarter century (Fig. **2**).

Human-made climate change is delayed by ocean (Fig. **S7**) and ice sheet response times. Warming 'in the pipeline', mostly attributable to slow feedbacks, is now about 2°C (Fig. **2**). No additional forcing is required to raise global temperature to at least the level of the Pliocene, 2-3 million years ago, a degree of warming that would surely yield 'dangerous' climate impacts [5].

4.1. Tipping Points

Realization that today's climate is far out of equilibrium with current climate forcings raises the specter of 'tipping points', the concept that climate can reach a point where, without additional forcing, rapid changes proceed practically out of our control [2, 7, 63, 64]. Arctic sea ice and the West Antarctic Ice Sheet are examples of potential tipping points. Arctic sea ice loss is magnified by the positive feedback of increased absorption of sunlight as global warming initiates sea ice retreat [65]. West Antarctic ice loss can be accelerated by several feedbacks, once ice loss is substantial [39].

We define: (1) the *tipping level*, the global climate forcing that, if long maintained, gives rise to a specific consequence, and (2) the *point of no return*, a climate state beyond which the consequence is inevitable, even if climate forcings are reduced. A point of no return can be avoided, even if the tipping level is temporarily exceeded. Ocean and ice sheet inertia permit overshoot, provided the climate forcing is returned below the tipping level before initiating irreversible dynamic change.

Points of no return are inherently difficult to define, because the dynamical problems are nonlinear. Existing models are more lethargic than the real world for phenomena now unfolding, including changes of sea ice [65], ice streams [66], ice shelves [36], and expansion of the subtropics [67, 68].

The tipping level is easier to assess, because the paleoclimate quasi-equilibrium response to known climate forcing is relevant. The tipping level is a measure of the long-term climate forcing that humanity must aim to stay beneath to avoid large climate impacts. The tipping level does not define the magnitude or period of tolerable overshoot. However, if overshoot is in place for centuries, the thermal per-

turbation will so penetrate the ocean [10] that recovery without dramatic effects, such as ice sheet disintegration, becomes unlikely.

4.2. Target CO_2

Combined, GHGs other than CO_2 cause climate forcing comparable to that of CO_2 [2, 6], but growth of non-CO_2 GHGs is falling below IPCC [2] scenarios. Thus total GHG climate forcing change is now determined mainly by CO_2 [69]. Coincidentally, CO_2 forcing is similar to the net human-made forcing, because non-CO_2 GHGs tend to offset negative aerosol forcing [2, 5].

Thus we take future CO_2 change as approximating the net human-made forcing change, with two caveats. First, special effort to reduce non-CO_2 GHGs could alleviate the CO_2 requirement, allowing up to about +25 ppm CO_2 for the same climate effect, while resurgent growth of non-CO_2 GHGs could reduce allowed CO_2 a similar amount [6]. Second, reduction of human-made aerosols, which have a net cooling effect, could force stricter GHG requirements. However, an emphasis on reducing black soot could largely off-set reductions of high albedo aerosols [20].

Our estimated history of CO_2 through the Cenozoic Era provides a sobering perspective for assessing an appropriate target for future CO_2 levels. A CO_2 amount of order 450 ppm or larger, if long maintained, would push Earth toward the ice-free state. Although ocean and ice sheet inertia limit the rate of climate change, such a CO_2 level likely would cause the passing of climate tipping points and initiate dynamic responses that could be out of humanity's control.

The climate system, because of its inertia, has not yet fully responded to the recent increase of human-made climate forcings [5]. Yet climate impacts are already occurring that allow us to make an initial estimate for a target atmospheric CO_2 level. No doubt the target will need to be adjusted as climate data and knowledge improve, but the urgency and difficulty of reducing the human-made forcing will be less, and more likely manageable, if excess forcing is limited soon.

Civilization is adapted to climate zones of the Holocene. Theory and models indicate that subtropical regions expand poleward with global warming [2, 67]. Data reveal a 4-degree latitudinal shift already [68], larger than model predictions, yielding increased aridity in southern United States [70, 71], the Mediterranean region, Australia and parts of Africa. Impacts of this climate shift [72] support the conclusion that 385 ppm CO_2 is already deleterious.

Alpine glaciers are in near-global retreat [72, 73]. After a one-time added flush of fresh water, glacier demise will yield summers and autumns of frequently dry rivers, including rivers originating in the Himalayas, Andes and Rocky Mountains that now supply water to hundreds of millions of people. Present glacier retreat, and warming in the pipeline, indicate that 385 ppm CO_2 is already a threat.

Equilibrium sea level rise for today's 385 ppm CO_2 is at least several meters, judging from paleoclimate history [19, 32-34]. Accelerating mass losses from Greenland [74] and West Antarctica [75] heighten concerns about ice sheet stability. An initial CO_2 target of 350 ppm, to be reassessed as effects on ice sheet mass balance are observed, is suggested.

Stabilization of Arctic sea ice cover requires, to first approximation, restoration of planetary energy balance. Climate models driven by known forcings yield a present planetary energy imbalance of +0.5-1 W/m^2 [5]. Observed heat increase in the upper 700 m of the ocean [76] confirms the planetary energy imbalance, but observations of the entire ocean are needed for quantification. CO_2 amount must be reduced to 325-355 ppm to increase outgoing flux 0.5-1 W/m^2, if other forcings are unchanged. A further imbalance reduction, and thus CO_2 ~300-325 ppm, may be needed to restore sea ice to its area of 25 years ago.

Coral reefs are suffering from multiple stresses, with ocean acidification and ocean warming principal among them [77]. Given additional warming 'in-the-pipeline', 385 ppm CO_2 is already deleterious. A 300-350 ppm CO_2 target would significantly relieve both of these stresses.

4.3. CO_2 Scenarios

A large fraction of fossil fuel CO_2 emissions stays in the air a long time, one-quarter remaining airborne for several centuries [11, 78, 79]. Thus moderate delay of fossil fuel use will not appreciably reduce long-term human-made climate change. Preservation of a climate resembling that to which humanity is accustomed, the climate of the Holocene, requires that most remaining fossil fuel carbon is never emitted to the atmosphere.

Coal is the largest reservoir of conventional fossil fuels (Fig. **S12**), exceeding combined reserves of oil and gas [2, 79]. The only realistic way to sharply curtail CO_2 emissions is to phase out coal use except where CO_2 is captured and sequestered.

Phase-out of coal emissions by 2030 (Fig. **6**) keeps maximum CO_2 close to 400 ppm, depending on oil and gas reserves and reserve growth. IPCC reserves assume that half of readily extractable oil has already been used (Figs. **6**, **S12**). EIA [80] estimates (Fig. **S12**) have larger reserves and reserve growth. Even if EIA estimates are accurate, the IPCC case remains valid if the most difficult to extract oil and gas is left in the ground, *via* a rising price on carbon emissions that discourages remote exploration and environmental regulations that place some areas off-limit. If IPCC gas reserves (Fig. **S12**) are underestimated, the IPCC case in Fig. (**6**) remains valid if the additional gas reserves are used at facilities where CO_2 is captured.

However, even with phase-out of coal emissions and assuming IPCC oil and gas reserves, CO_2 would remain above 350 ppm for more than two centuries. Ongoing Arctic and ice sheet changes, examples of rapid paleoclimate change, and other criteria cited above all drive us to consider scenarios that bring CO_2 more rapidly back to 350 ppm or less.

4.4. Policy Relevance

Desire to reduce airborne CO_2 raises the question of whether CO_2 could be drawn from the air artificially. There are no large-scale technologies for CO_2 air capture now, but

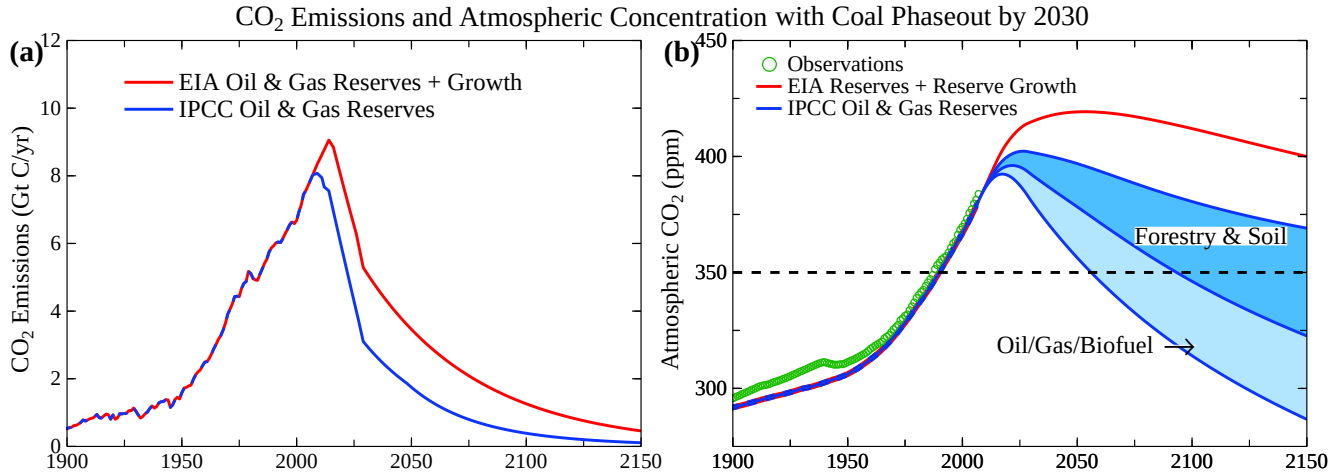

Fig. (6). (**a**) Fossil fuel CO_2 emissions with coal phase-out by 2030 based on IPCC [2] and EIA [80] estimated fossil fuel reserves. (**b**) Resulting atmospheric CO_2 based on use of a dynamic-sink pulse response function representation of the Bern carbon cycle model [78, 79].

with strong research and development support and industrial-scale pilot projects sustained over decades it may be possible to achieve costs ~$200/tC [81] or perhaps less [82]. At $200/tC, the cost of removing 50 ppm of CO_2 is ~$20 trillion.

Improved agricultural and forestry practices offer a more natural way to draw down CO_2. Deforestation contributed a net emission of 60±30 ppm over the past few hundred years, of which ~20 ppm CO_2 remains in the air today [2, 83] (Figs. (**S12**, **S14**). Reforestation could absorb a substantial fraction of the 60±30 ppm net deforestation emission.

Carbon sequestration in soil also has significant potential. Biochar, produced in pyrolysis of residues from crops, forestry, and animal wastes, can be used to restore soil fertility while storing carbon for centuries to millennia [84]. Biochar helps soil retain nutrients and fertilizers, reducing emissions of GHGs such as N_2O [85]. Replacing slash-and-burn agriculture with slash-and-char and use of agricultural and forestry wastes for biochar production could provide a CO_2 drawdown of ~8 ppm or more in half a century [85].

In the Supplementary Material Section we define a forest/soil drawdown scenario that reaches 50 ppm by 2150 (Fig. **6b**). This scenario returns CO_2 below 350 ppm late this century, after about 100 years above that level.

More rapid drawdown could be provided by CO_2 capture at power plants fueled by gas and biofuels [86]. Low-input high-diversity biofuels grown on degraded or marginal lands, with associated biochar production, could accelerate CO_2 drawdown, but the nature of a biofuel approach must be carefully designed [85, 87-89].

A rising price on carbon emissions and payment for carbon sequestration is surely needed to make drawdown of airborne CO_2 a reality. A 50 ppm drawdown *via* agricultural and forestry practices seems plausible. But if most of the CO_2 in coal is put into the air, no such "natural" drawdown of CO_2 to 350 ppm is feasible. Indeed, if the world continues on a business-as-usual path for even another decade without initiating phase-out of unconstrained coal use, prospects for avoiding a dangerously large, extended overshoot of the 350 ppm level will be dim.

4.5. Caveats: Climate Variability, Climate Models, and Uncertainties

Climate has great variability, much of which is unforced and unpredictable [2, 90]. This fact raises a practical issue: what is the chance that climate variations, e.g., a temporary cooling trend, will affect public recognition of climate change, making it difficult to implement mitigation policies? Also what are the greatest uncertainties in the expectation of a continued global warming trend? And what are the impacts of climate model limitations, given the inability of models to realistically simulate many aspects of climate change and climate processes?

The atmosphere and ocean exhibit coupled nonlinear chaotic variability that cascades to all time scales [91]. Variability is so large that the significance of recent decadal global temperature change (Fig. **7a**) would be very limited, if the data were considered simply as a time series, without further information. However, other knowledge includes information on the causes of some of the temperature variability, the planet's energy imbalance, and global climate forcings.

The El Nino Southern Oscillation (ENSO) [94] accounts for most low latitude temperature variability and much of the global variability. The global impact of ENSO is coherent from month to month, as shown by the global-ocean-mean SST (Fig. **7b**), for which the ocean's thermal inertia minimizes the effect of weather noise. The cool anomaly of 2008 coincides with an ENSO minimum and does not imply a change of decadal temperature trend.

Decadal time scale variability, such as predicted weakening of the Atlantic overturning circulation [95], could interrupt global warming, as discussed in section 18 of the Supplementary Material. But the impact of regional dynamical effects on global temperature is opposed by the planet's energy imbalance [96], a product of the climate system's thermal inertia, which is confirmed by increasing ocean heat

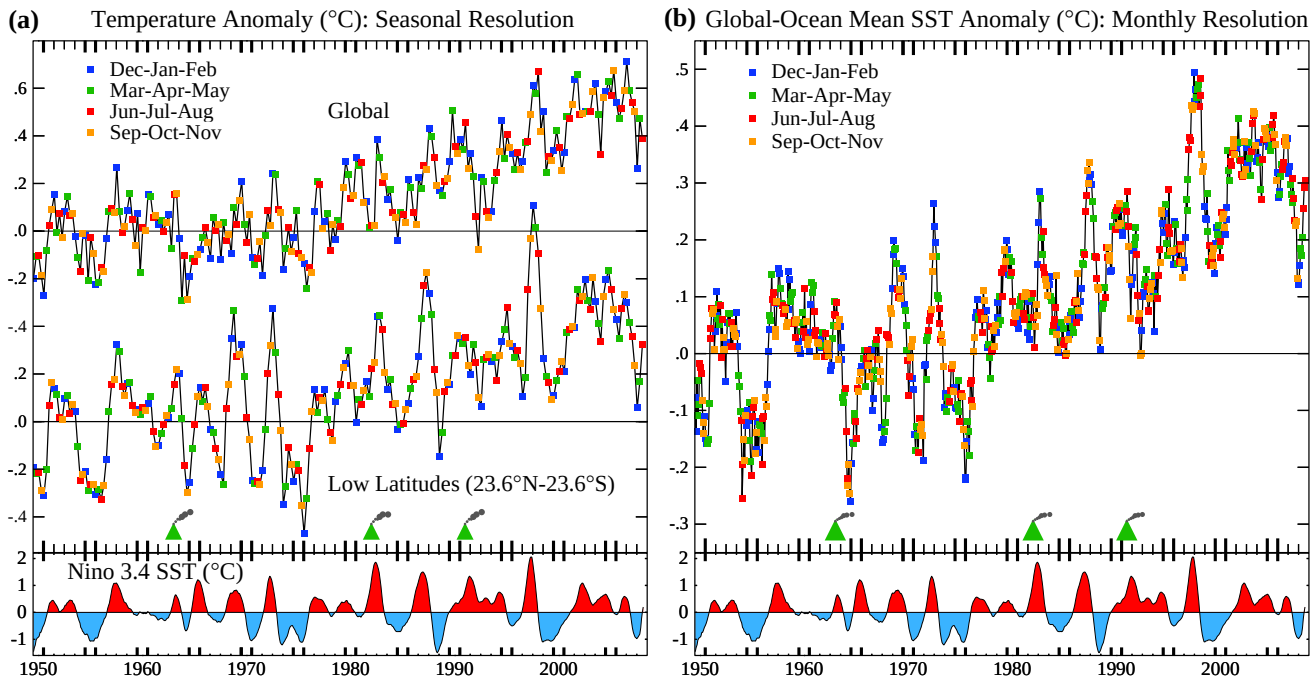

Fig. (7). (**a**) Seasonal-mean global and low-latitude surface temperature anomalies relative to 1951-1980, an update of [92], (**b**) global-ocean-mean sea surface temperature anomaly at monthly resolution. The Nino 3.4 Index, the temperature anomaly (12-month running mean) in a small part of the tropical Pacific Ocean [93], is a measure of ENSO, a basin-wide sloshing of the tropical Pacific Ocean [94]. Green triangles show major volcanic eruptions.

storage [97]. This energy imbalance makes decadal interruption of global warming, in the absence of a negative climate forcing, improbable [96].

Volcanoes and the sun can cause significant negative forcings. However, even if the solar irradiance remained at its value in the current solar minimum, this reduced forcing would be offset by increasing CO_2 within seven years (Supplementary Material section 18). Human-made aerosols cause a greater negative forcing, both directly and through their effects on clouds. The first satellite observations of aerosols and clouds with accuracy sufficient to quantify this forcing are planned to begin in 2009 [98], but most analysts anticipate that human-made aerosols will decrease in the future, rather than increase further.

Climate models have many deficiencies in their abilities to simulate climate change [2]. However, model uncertainties cut both ways: it is at least as likely that models underestimate effects of human-made GHGs as overestimate them (Supplementary Material section 18). Model deficiencies in evaluating tipping points, the possibility that rapid changes can occur without additional climate forcing [63, 64], are of special concern. Loss of Arctic sea ice, for example, has proceeded more rapidly than predicted by climate models [99]. There are reasons to expect that other nonlinear problems, such as ice sheet disintegration and extinction of interdependent species and ecosystems, also have the potential for rapid change [39, 63, 64].

5. SUMMARY

Humanity today, collectively, must face the uncomfortable fact that industrial civilization itself has become the principal driver of global climate. If we stay our present course, using fossil fuels to feed a growing appetite for energy-intensive life styles, we will soon leave the climate of the Holocene, the world of prior human history. The eventual response to doubling pre-industrial atmospheric CO_2 likely would be a nearly ice-free planet, preceded by a period of chaotic change with continually changing shorelines.

Humanity's task of moderating human-caused global climate change is urgent. Ocean and ice sheet inertias provide a buffer delaying full response by centuries, but there is a danger that human-made forcings could drive the climate system beyond tipping points such that change proceeds out of our control. The time available to reduce the human-made forcing is uncertain, because models of the global system and critical components such as ice sheets are inadequate. However, climate response time is surely less than the atmospheric lifetime of the human-caused perturbation of CO_2. Thus remaining fossil fuel reserves should not be exploited without a plan for retrieval and disposal of resulting atmospheric CO_2.

Paleoclimate evidence and ongoing global changes imply that today's CO_2, about 385 ppm, is already too high to maintain the climate to which humanity, wildlife, and the rest of the biosphere are adapted. Realization that we must reduce the current CO_2 amount has a bright side: effects that had begun to seem inevitable, including impacts of ocean acidification, loss of fresh water supplies, and shifting of climatic zones, may be averted by the necessity of finding an energy course beyond fossil fuels sooner than would otherwise have occurred.

We suggest an initial objective of reducing atmospheric CO_2 to 350 ppm, with the target to be adjusted as scientific understanding and empirical evidence of climate effects accumulate. Although a case already could be made that the eventual target probably needs to be lower, the 350 ppm target is sufficient to qualitatively change the discussion and drive fundamental changes in energy policy. Limited opportunities for reduction of non-CO_2 human-caused forcings are important to pursue but do not alter the initial 350 ppm CO_2 target. This target must be pursued on a timescale of decades, as paleoclimate and ongoing changes, and the ocean response time, suggest that it would be foolhardy to allow CO_2 to stay in the dangerous zone for centuries.

A practical global strategy almost surely requires a rising global price on CO_2 emissions and phase-out of coal use except for cases where the CO_2 is captured and sequestered. The carbon price should eliminate use of unconventional fossil fuels, unless, as is unlikely, the CO_2 can be captured. A reward system for improved agricultural and forestry practices that sequester carbon could remove the current CO_2 overshoot. With simultaneous policies to reduce non-CO_2 greenhouse gases, it appears still feasible to avert catastrophic climate change.

Present policies, with continued construction of coal-fired power plants without CO_2 capture, suggest that decision-makers do not appreciate the gravity of the situation. We must begin to move now toward the era beyond fossil fuels. Continued growth of greenhouse gas emissions, for just another decade, practically eliminates the possibility of near-term return of atmospheric composition beneath the tipping level for catastrophic effects.

The most difficult task, phase-out over the next 20-25 years of coal use that does not capture CO_2, is Herculean, yet feasible when compared with the efforts that went into World War II. The stakes, for all life on the planet, surpass those of any previous crisis. The greatest danger is continued ignorance and denial, which could make tragic consequences unavoidable.

ACKNOWLEDGMENTS

We thank H. Harvey and Hewlett Foundation, G. Lenfest, the Rockefeller Family Foundation, and NASA program managers D. Anderson and J. Kaye for research support, an anonymous reviewer, S. Baum, B. Brook, P. Essunger, K. Farnish, Q. Fu, L.D. Harvey, I. Horovitz, R. Keeling, C. Kutscher, J. Leventhal, C. McGrath, T. Noerpel, P. Read, J. Romm, D. Sanborn, S. Schwartz, J. Severinghaus, K. Ward and S. Weart for comments on a draft manuscript, G. Russell for the computations in Fig. (**S3**), and T. Conway and P. Tans of NOAA Earth System Research Laboratory and R. Andres, T. Boden and G. Marland of DOE CDIAC for data.

REFERENCES

[1] Framework Convention on Climate Change, United Nations 1992; http://www.unfccc.int/

[2] Intergovernmental Panel on Climate Change (IPCC), Climate Change 2007, Solomon S, Dahe Q, Manning M, *et al.* (eds), Cambridge Univ Press: New York 2007; pp. 996.

[3] Mastrandrea MD, Schneider SH. Probabilistic integrated assessment of "dangerous" climate change. Science 2004; 304: 571-5.

[4] European Council, Climate change strategies 2005; http://register.consilium.europa.eu/pdf/en/05/st07/st07242.en05.pdf

[5] Hansen J, Sato M, Ruedy, *et al.* Dangerous human-made interference with climate: a GISS modelE study. Atmos Chem Phys 2007; 7: 2287-312.

[6] Hansen J, Sato M. Greenhouse gas growth rates. Proc Natl Acad Sci 2004; 101: 16109-14.

[7] Hansen J, Sato M, Kharecha P, Russell G, Lea DW, Siddall M. Climate change and trace gases. Phil Trans R Soc A 2007; 365: 1925-54.

[8] Hansen J, Nazarenko L, Ruedy R, *et al.* Earth's energy imbalance: Confirmation and implications. Science 2005; 308: 1431-35.

[9] Harvey LDD. Dangerous anthropogenic interference, dangerous climatic change, and harmful climatic change: non-trivial distinctions with significant policy implications. Clim Change 2007; 82: 1-25.

[10] Matthews HD, Caldeira K. Stabilizing climate requires near-zero emissions. Geophys Res Lett 2008; 35: L04705.

[11] Archer D. Fate of fossil fuel CO_2 in geologic time. J Geophys Res 2005; 110: C09S05.

[12] Hansen J, Sato M, Ruedy R, *et al.* Efficacy of climate forcings. J Geophys Res 2005; 110: D18104.

[13] Charney J. Carbon Dioxide and Climate: A Scientific Assessment. National Academy of Sciences Press: Washington DC 1979; pp. 33.

[14] Hansen J, Lacis A, Rind D, *et al.* J Climate sensitivity: Analysis of feedback mechanisms. In Climate Processes and Climate Sensitivity, Geophys Monogr Ser 29. Hansen JE, Takahashi T, Eds. American Geophysical Union: Washington, DC 1984; pp. 130-63.

[15] Braconnot P, Otto-Bliesner BL, Harrison S, *et al.* Results of PMIP2 coupled simulations of the Mid-Holocene and Last Glacial Maximum – Part 1: experiments and large-scale features. Clim Past 2007; 3: 261-77.

[16] Farrera I, Harrison SP, Prentice IC, *et al.* Tropical climates at the last glacial maximum: a new synthesis of terrestrial paeleoclimate data. I. Vegetation, lake-levels and geochemistry. Clim Dyn 1999; 15: 823-56

[17] Petit JR, Jouzel J, Raynaud D, *et al.* 420,000 years of climate and atmospheric history revealed by the Vostok deep Antarctic ice core. Nature 1999; 399: 429-36.

[18] Vimeux F, Cuffey KM, Jouzel J. New insights into Southern Hemisphere temperature changes from Vostok ice cores using deuterium excess correction. Earth Planet Sci Lett 2002; 203: 829-43.

[19] Siddall M, Rohling EJ, Almogi-Labin A, *et al.* Sea-level fluctuations during the last glacial cycle. Nature 2003; 423: 853-58.

[20] Hansen J, Sato M, Ruedy R, Lacis A, Oinas V. Global warming in the twenty-first century: An alternative scenario. Proc Natl Acad Sci 2000; 97: 9875-80.

[21] Masson-Delmotte V, Kageyama M, Braconnot P. Past and future polar amplification of climate change: climate model intercomparisons and ice-core constraints. Clim Dyn 2006; 26: 513-29.

[22] EPICA community members. One-to-one coupling of glacial climate variability in Greenland and Antarctica. Nature 2006; 444: 195-8.

[23] Caillon N, Severinghaus JP, Jouzel J, Barnola JM, Kang J, Lipenkov VY. Timing of atmospheric CO_2 and Antarctic temperature changes across Termination III. Science 2003; 299: 1728-31.

[24] Mudelsee M. The phase relations among atmospheric CO_2 content, temperature and global ice volume over the past 420 ka. Quat Sci Rev 2001; 20: 583-9.

[25] Hays JD, Imbrie J, Shackleton NJ. Variations in the Earth's orbit: pacemaker of the ice ages. Science 1976; 194: 1121-32.

[26] Zachos J, Pagani M, Sloan L, Thomas E, Billups K. Trends, rhythms, and aberrations in global climate 65 Ma to present. Science 2001; 292: 686-93.

[27] Kohler P, Fischer H. Simulating low frequency changes in atmospheric CO_2 during the last 740 000 years. Clim Past 2006; 2: 57-78.

[28] Siegenthaler U, Stocker TF, Monnin E, *et al.* Stable carbon cycle – climate relationship during the late Pleistocene. Science 2005; 310: 1313-7.

[29] Archer D. Methane hydrate stability and anthropogenic climate change. Biogeoscience 2007; 4: 521-44.

[30] Berner RA. The Phanerozoic Carbon Cycle: CO_2 and O_2; Oxford Univ Press: New York 2004; p. 150.

[31] Hansen J, Russell G, Lacis A, *et al.* Climate response times: Dependence on climate sensitivity and ocean mixing. Science 1985; 229: 857-9.

[32] Thompson WG, Goldstein SL. Open-system coral ages reveal persistent suborbital sea-level cycles. Science 2005; 308: 401-4.

[33] Hearty PJ, Hollin JT, Neumann AC, O'Leary MJ, McCulloch M. Global sea-level fluctuations during the last interglaciation (MIS 5e). Quat Sci Rev 2007; 26: 2090-112.

[34] Rohling EJ, Grant K, Hemleben Ch, *et al* . High rates of sea-level rise during the last interglacial period. Nat Geosci 2008; 1: 38-42.

[35] Tedesco M. Snowmelt detection over the Greenland ice sheet from SSM/I brightness temperature daily variations. Geophys Res Lett 2007; 34: L02504, 1-6.

[36] Rignot E, Jacobs SS. Rapid bottom melting widespread near Antarctic ice sheet grounding lines. Science 2002; 296: 2020-3.

[37] Zwally HJ, Abdalati W, Herring T, Larson K, Saba J, Steffen K. Surface melt-induced acceleration of Greenland ice-sheet flow. Science 2002; 297: 218-22.

[38] Chen JL, Wilson CR, Tapley BD. Satellite gravity measurements confirm accelerated melting of Greenland Ice Sheet. Science 2006; 313: 1958-60.

[39] Hansen J. A slippery slope: how much global warming constitutes "dangerous anthropogenic interference"? Clim Change 2005; 68: 269-79.

[40] DeConto RM, Pollard D. Rapid Cenozoic glaciation of Antarctica induced by declining atmospheric CO_2. Nature 2003; 421: 245-9.

[41] Zanazzi A, Kohn MJ, MacFadden BJ, Terry DO. Large temperature drop across the Eocene-Oligocene transition in central North America. Nature 2007; 445: 639-42.

[42] Dupont-Nivet G, Krijgsman W, Langereis CG, Abeld HA, Dai S, Fang X. Tibetan plateau aridification linked to global cooling at the Eocene–Oligocene transition. Nature 2007; 445: 635-8.

[43] Sackmann IJ, Boothroyd AI, Kraemer KE. Our sun III Present and future. Astrophys J 1993; 418: 457-68.

[44] Pagani M, Zachos J, Freeman KH, Bohaty S, Tipple B. Marked change in atmospheric carbon dioxide concentrations during the Oligocene. Science 2005; 309: 600-3.

[45] Bartdorff O, Wallmann K, Latif M, Semenov V. Phanerozoic evolution of atmospheric methane. Global Biogeochem Cycles 2008; 22: GB1008.

[46] Beerling D, Berner RA, Mackenzie FT, Harfoot MB, Pyle JA. Methane and the CH_4 greenhouse during the past 400 million years. Am J Sci 2008; (in press).

[47] Edmond JM, Huh Y. Non-steady state carbonate recycling and implications for the evolution of atmospheric P_{CO2}. Earth Planet Sci Lett 2003; 216: 125-39.

[48] Staudigel H, Hart SR, Schmincke H-U, Smith BM. Cretaceous ocean crust at DSDP Sites 417 and 418: Carbon uptake from weathering versus loss by magmatic outgassing. Geochim Cosmochim Acta 1989; 53: 3091-4.

[49] Berner R, Caldeira K. The need for mass balance and feedback in the geochemical carbon cycle. Geology 1997; 25: 955-6.

[50] Kumar P, Yuan X, Kumar MR, Kind R, Li X, Chadha RK. The rapid drift of the Indian tectonic plate. Nature 2007; 449: 894-97.

[51] Raymo ME, Ruddiman WF. Tectonic forcing of late Cenozoic climate. Nature 1992; 359: 117-22.

[52] Zeebe RE, Caldeira K. Close mass balance of long-term carbon fluxes from ice-core CO_2 and ocean chemistry records. Nat Geosci 2008; 1: 312-5.

[53] Patriat P, Sloan H, Sauter D. From slow to ultraslow: a previously undetected event at the Southwest Indian Ridge at ca. 24 Ma. Geology 2008; 36: 207-10.

[54] Joshi MM, Gregory JM, Webb MJ, Sexton DMH, Johns TC. Mechanisms for the land/sea warming contrast exhibited by simulations of climate change. Clim Dyn 2008; 30: 455-65.

[55] Royer DL. CO_2-forced climate thresholds during the Phanerozoic. Geochim Cosmochim Acta 2006; 70: 5665-75.

[56] Royer DL, Berner RA, Park J. Climate sensitivity constrained by CO_2 concentrations over the past 420 million years. Nature 2007; 446: 530-2.

[57] Higgins JA, Schrag DP. Beyond methane: Towards a theory for Paleocene-Eocene thermal maximum. Earth Planet Sci Lett 2006; 245: 523-37.

[58] Pagani M, Caldeira K, Archer D, Zachos JC. An ancient carbon mystery. Science 2006; 314: 1556-7.

[59] Lunt DJ, Valdes PJ, Haywood A, Rutt IC. Closure of the Panama Seaway during the Pliocene: implications for climate and Northern Hemisphere glaciation. Clim Dyn 2008; 30: 1-18.

[60] Crutzen PJ, Stoermer EF. The "Anthropocene". Glob Change Newslett 2000; 41: 12-3.

[61] Zalasiewicz J, Williams M, Smith A, *et al.* Are we now living in the Anthropocene? GSA Today 2008; 18: 4-8.

[62] Ruddiman WF. The anthropogenic greenhouse era began thousands of years ago. Clim Change 2003; 61: 261-93.

[63] Hansen J. Tipping point: perspective of a climatologist. In State of the Wild: A Global Portrait of Wildlife, Wildlands, and Oceans. Woods W, Ed. Wildlife Conservation Society/Island Press 2008; pp. 6-15.

[64] Lenton TM, Held H, Kriegler E, *et al.* Tipping elements in the Earth's climate system. Proc Natl Acad Sci USA 2008; 105: 1786-93.

[65] Stroeve J, Serreze M, Drobot S, *et al*. Arctic sea ice extent plummets in 2007. Eos Trans, AGU 2008; 89(2): 13.

[66] Howat IM, Joughin I, Scambos TA. Rapid changes in ice discharge from Greenland outlet glaciers. Science 2007; 315: 1559-61.

[67] Held IM, Soden BJ. Robust responses of the hydrological cycle to global warming. J Clim 2006; 19: 5686-99.

[68] Seidel DJ, Randel WJ. Variability and trends in the global tropopause estimated from radiosonde data. J Geophys Res 2006; 111: D21101.

[69] Hansen J, Sato M. Global warming: East-West connections. Open Environ J 2008; (in press).

[70] Barnett TP, Pierce DW, Hidalgo HG, *et al.* Human-induced changes in the hydrology of the Western United States. Science 2008; 319: 1080-3.

[71] Levi BG. Trends in the hydrology of the western US bear the imprint of manmade climate change. Phys Today 2008; April: 16-8.

[72] Intergovernmental Panel on Climate Change (IPCC), Impacts, Adaptation and Vulnerability. Parry M, Canziani O, Palutikof J, van der Linden P, Hanson C, Eds. Cambridge Univ. Press: New York 2007; pp. 978.

[73] Barnett TP, Adam JC, Lettenmaler DP. Potential impacts of a warming climate on water availability in snow-dominated regions. Nature 2005; 438: 303-9.

[74] Steffen K, Clark PU, Cogley JG, Holland D, Marshall S, Rignot E, Thomas R. Rapid changes in glaciers and ice sheets and their impacts on sea level. Chap. 2 in Abrupt Climate Change, U.S. Climate Change Science Program, SAP-3.4 2008; pp. 452.

[75] Rignot E, Bamber JL, van den Broeke MR, *et al*. Recent Antarctic ice mass loss from radar interferometry and regional climate modeling. Nat Geosci 2008; 1: 106-10.

[76] Domingues CM, Church JA, White NJ, *et al*. Rapid upper-ocean warming helps explain multi-decadal sea-level rise. Nautre 2008; (in press).

[77] Stone R. A world without corals? Science 2007; 316: 678-81.

[78] Joos F, Bruno M, Fink R, *et al*. An efficient and accurate representation of complex oceanic and biospheric models of anthropogenic carbon uptake. Tellus B 1996; 48: 397-17.

[79] Kharecha P, Hansen J. Implications of "peak oil" for atmospheric CO_2 and climate. Global Biogeochem Cycles 2008; 22: GB3012.

[80] Energy Information Administration (EIA), U.S. DOE, International Energy Outlook 2006, http://www.eia.doe.gov/oiaf/archive/ieo06/index.html

[81] Keith DW, Ha-Duong M, Stolaroff JK. Climate strategy with CO_2 capture from the air. Clim Change 2006; 74: 17-45.

[82] Lackner KS. A guide to CO_2 sequestration. Science 2003; 300: 1677-8.

[83] Houghton RA. Revised estimates of the annual net flux of carbon to the atmosphere from changes in land use and land management 1850-2000. Tellus B 2003; 55: 378-90.

[84] Lehmann J. A handful of carbon. Nature 2007; 447: 143-4.

[85] Lehmann J, Gaunt J, Rondon M. Bio-char sequestration in terrestrial ecosystems – a review. Mitig Adapt Strat Glob Change 2006; 11: 403-27.

[86] Hansen J. Congressional Testimony 2007; http://arxiv.org/abs/0706.3720v1

[87] Tilman D, Hill J, Lehman C. Carbon-negative biofuels from low-input high-diversity grassland biomass. Science 2006; 314: 1598-600.

[88] Fargione J, Hill J, Tilman D, Polasky S, Hawthorne P. Land clearing and the biofuel carbon debt. Science 2008; 319: 1235-8.

[89] Searchinger T, Heimlich R, Houghton RA, *et al* . Use of U.S. croplands for biofuels increases greenhouse gases through emissions from land-use change. Science 2008; 319: 1238-40.
[90] Palmer TN. Nonlinear dynamics and climate change: Rossby's legacy. Bull Am Meteorol Soc 1998; 79: 1411-23.
[91] Hasselmann K. Ocean circulation and climate change. Tellus B 2002; 43: 82-103.
[92] Hansen J, Ruedy R, Glascoe J, Sato M. GISS analysis of surface temperature change. J Geophys Res 1999; 104: 30997-1022.
[93] NOAA National Weather Service, Climate prediction Center 2008; http://www.cpc.ncep.noaa.gov/data/indices/sstoi.indices
[94] Cane MA. Nino E. Ann Rev Earth Planet Sci 1986; 14: 43-70.
[95] Keenlyside NS, Latif M, Jungclaus J, Kornblueh L, Roeckner E. Advancing decadal-scale climate prediction in the North Atlantic sector. Nature 2008; 453: 84-8.
[96] Hansen J, Sato M, Ruedy R, *et al.* Forcings and chaos in interannual to decadal climate change. J Geophys Res 1997; 102: 25679-720.
[97] Domingues CM, Church JA, White NJ, *et al*. Improved estimates of upper-ocean warming and multi-decadal sea-level rise. Nature 2008; 453: 1090-3.
[98] Mishchenko MI, Cairns B, Kopp G, *et al* . Precise and accurate monitoring of terrestrial aerosols and total solar irradiance: introducing the Glory mission. Bull Am Meteorol Soc 2007; 88: 677-91.
[99] Lindsay RW, Zhang J. The Thinning of Arctic Sea Ice, 1988–2003: Have we passed a tipping point? J Clim 2005; 18: 4879-94.

Received: May 22, 2008 Revised: August 19, 2008 Accepted: September 23, 2008

Supplementary Material

1. ICE AGE CLIMATE FORCINGS

Fig. (**S1**) shows the climate forcings during the depth of the last ice age, 20 ky BP, relative to the Holocene [14]. The largest contribution to the uncertainty in the calculated 3.5 W/m^2 forcing due to surface changes (ice sheet area, vegetation distribution, shoreline movements) is due to uncertainty in the ice sheet sizes [14, S1]. Formulae for the GHG forcings [20] yield 2.25 W/m^2 for CO_2 (185 ppm → 275 ppm), 0.43 W/m^2 for CH_4 (350 → 675 ppb) and 0.32 W/m^2 for N_2O (200 → 270 ppb). The CH_4 forcing includes a factor 1.4 to account for indirect effects of CH_4 on tropospheric ozone and stratospheric water vapor [12].

The climate sensitivity inferred from the ice age climate change (~¾°C per W/m^2) includes only fast feedbacks, such as water vapor, clouds, aerosols (including dust) and sea ice. Ice sheet size and greenhouse gas amounts are specified boundary conditions in this derivation of the fast-feedback climate sensitivity.

It is permissible, alternatively, to specify aerosol changes as part of the forcing and thus derive a climate sensitivity that excludes the effect of aerosol feedbacks. That approach was used in the initial empirical derivation of climate sensitivity from Pleistocene climate change [14]. The difficulty with that approach is that, unlike long-lived GHGs, aerosols are distributed heterogeneously, so it is difficult to specify aerosol changes accurately. Also the forcing is a sensitive function of aerosol single scatter albedo and the vertical distribution of aerosols in the atmosphere, which are not measured. Furthermore, the aerosol indirect effect on clouds also depends upon all of these poorly known aerosol properties.

One recent study [S2] specified an arbitrary glacial-interglacial aerosol forcing slightly larger than the GHG glacial-interglacial forcing. As a result, because temperature, GHGs, and aerosol amount, overall, are positively correlated in glacial-interglacial changes, this study inferred a climate sensitivity of only ~2°C for doubled CO_2. This study used the correlation of aerosol and temperature in the Vostok ice core at two specific times to infer an aerosol forcing for a given aerosol amount. The conclusions of the study are immediately falsified by considering the full Vostok aerosol record (Fig. **2** of [17]), which reveals numerous large aerosol fluctuations without any corresponding temperature change. In contrast, the role of GHGs in climate change is confirmed when this same check is made for GHGs (Fig. **2**), and the fast-feedback climate sensitivity of 3°C for doubled CO_2 is confirmed (Fig. **1**).

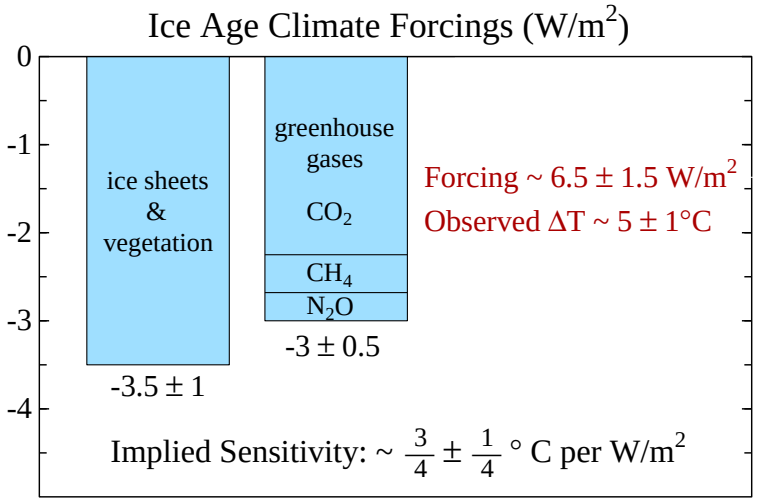

Fig. (S1). Climate forcings during ice age 20 ky BP, relative to the present (pre-industrial) interglacial period.

All the problems associated with imprecise knowledge of aerosol properties become moot if, as is appropriate, aerosols are included in the fast feedback category. Indeed, soil dust, sea salt, dimethylsulfide, and other aerosols are expected to vary (in regional, inhomogeneous ways) as climate changes. Unlike long-lived GHGs, global aerosol amounts cannot be inferred from ice cores. But the effect of aerosol changes is fully included in observed global temperature change. The climate sensitivity that we derive in Fig. (**S1**) includes the aerosol effect accurately, because both the climate forcings and the global climate response are known. The indirect effect of aerosol change on clouds is, of course, also included precisely.

2. CLIMATE FORCINGS AND CLIMATE FEEDBACKS

The Earth's temperature at equilibrium is such that the planet radiates to space (as heat, i.e., infrared radiation) the same amount of energy that it absorbs from the sun, which is ~240 W/m^2. A blackbody temperature of ~255°K yields a heat flux of 240 W/m^2. Indeed, 255°K is the temperature in the mid-troposphere, the mean level of infrared emission to space.

A climate forcing is a perturbation to the planet's energy balance, which causes the Earth's temperature to change as needed to restore energy balance. Doubling atmospheric CO_2 causes a planetary energy imbalance of ~4 W/m^2, with more energy

coming in than going out. Earth's temperature would need to increase by ΔT_O = 1.2-1.3°C to restore planetary energy balance, if the temperature change were uniform throughout the atmosphere and if nothing else changed.

Actual equilibrium temperature change in response to any forcing is altered by feedbacks that can amplify or diminish the response, thus the mean surface temperature change is [14]

$$\Delta T_{eq} = f\,\Delta T_O$$
$$= \Delta T_O + \Delta T_{feedbacks}$$
$$= \Delta T_O + \Delta T_1 + \Delta T_2 + \ldots,$$

where f is the net feedback factor and the ΔT_i are increments due to specific feedbacks.

The role of feedback processes is clarified by defining the gain, g,

$$g = \Delta T_{feedbacks}/\Delta T_{eq}$$
$$= (\Delta T_1 + \Delta T_2 + \ldots)/\Delta T_{eq}$$
$$= g_1 + g_2 + \ldots$$

g_i is positive for an amplifying feedback and negative for a feedback that diminishes the response. The additive nature of the g_i, unlike f_i, is a useful characteristic of the gain. Evidently

$$f = 1/(1 - g)$$

The value of g (or f) depends upon the climate state, especially the planetary temperature. For example, as the planet becomes so warm that land ice disappears, the land ice albedo feedback diminishes, i.e. $g_{land\ ice\ albedo} \rightarrow 0$.

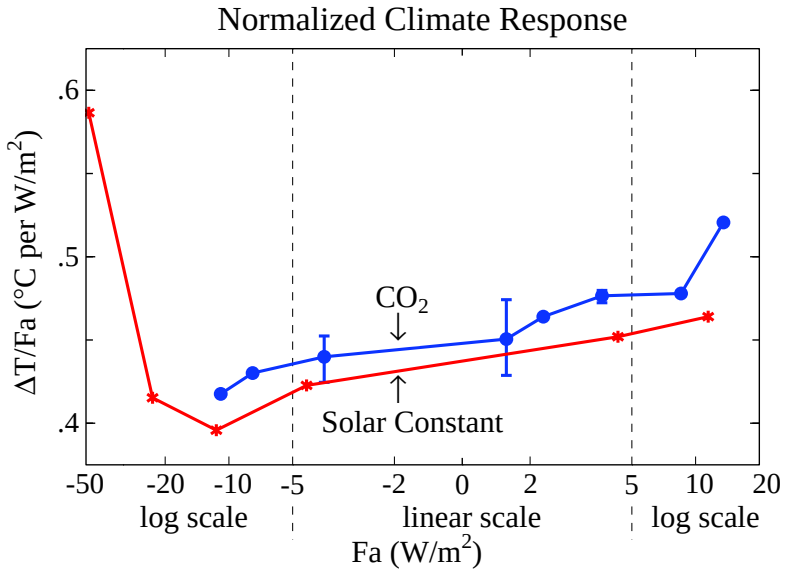

Fig. (S2). Global surface air temperature change [12] after 100 years in simulations with the Goddard Institute for Space Studies modelE [S3, 5] as a function of climate forcing for changes of solar irradiance and atmospheric CO_2. Fa is the standard adjusted climate forcing [12]. Results are extracted from Fig. (**25a**) of [12]. Curves terminate because the climate model 'bombs' at the next increment of forcing due to failure of one or more of the parameterizations of processes in the model as extreme conditions are approached.

'Fast feedbacks', such as water vapor, clouds and sea ice, are the mechanisms usually included in the 'Charney' [13] climate sensitivity. Climate models yield a Charney (fast feedback) sensitivity of about 3°C for doubled CO_2 [2, 12], a conclusion that is confirmed and tightened by empirical evidence from the Pleistocene (Section 2.1). This sensitivity implies

$$g_{fast\ feedbacks} \sim 0.5\text{-}0.6.$$

This fast feedback gain and climate sensitivity apply to the present climate and climate states with global temperatures that are not too different than at present.

If g approaches unity, $f \rightarrow \infty$, implying a runaway climate instability. The possibility of such instability is anticipated for either a very warm climate (runaway greenhouse effect [S4]) or a very cold climate (snowball Earth [S5]). We can investigate how large a climate forcing is needed to cause $g \rightarrow 1$ using a global climate model that includes the fast feedback processes, because both of these instabilities are a result of the temperature dependence of 'fast feedbacks' (the water vapor and ice/snow albedo feedbacks, respectively).

Fig. (**S2**) suggests that climate forcings ~10-25 W/m^2 are needed to approach either runaway snowball-Earth conditions or the runaway greenhouse effect. More precise quantification requires longer simulations and improved parameterizations of physical processes as extreme climates are approached. The processes should include slow feedbacks that can either amplify or diminish the climate change.

Earth has experienced snowball conditions [S5], or at least a 'slushball' state [S6] with ice reaching sea level in the tropics, on at least two occasions, the most recent ~640 My BP, aided by reduced solar irradiance [43] and favorable continental locations. The mechanism that allowed Earth to escape the snowball state was probably reduced weathering in a glaciated world, which allowed CO_2 to accumulate in the atmosphere [S5]. Venus, but not Earth, has experienced the runaway greenhouse effect, a state from which there is no escape.

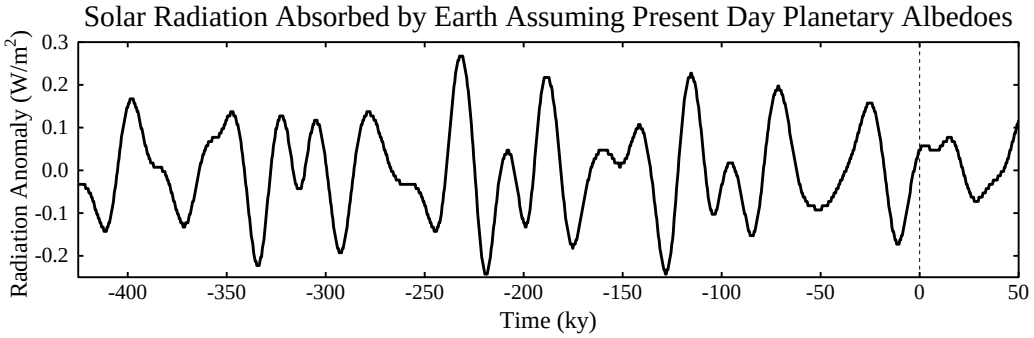

Fig. (S3). Annual-mean global-mean perturbation of the amount of solar radiation absorbed by the Earth, calculated by assuming present-day seasonal and geographical distribution of albedo.

3. PLEISTOCENE FORCINGS AND FEEDBACKS

Fig. (**S3**) shows the perturbation of solar radiation absorbed by the Earth due to changes in Earth orbital elements, i.e., the tilt of the Earth's spin axis relative to the orbital plane, the eccentricity of the Earth's orbit, and the time of year at which the Earth is closest to the sun (precession of equinoxes). This perturbation is calculated using fixed (present day) seasonal and geographical distribution of planetary albedo.

The global-mean annual-mean orbital (Milankovitch) forcing is very weak, at most a few tenths of 1 W/m^2. Our procedure in calculating the forcing, keeping ice sheet properties (size and albedo) fixed, is appropriate for 'instantaneous' and 'adjusted' radiative forcings [12].

Further, successive, definitions of the orbital 'forcing', e.g., allowing some regional response to the seasonal insolation perturbations, may be useful for the purpose of understanding glacial-interglacial climate change. For example, it may be informative to calculate the 'forcing' due to insolation-induced changes of ice-she*et al*bedo, because increased insolation can 'age' (increase snow crystal size and thus darken) an ice surface and also spur the date of first snow-melt [7]. However, one merit of the standard forcing definition is the insight that glacial-interglacial climate swings are almost entirely due to feedbacks.

Indeed, the gain during the Pleistocene is close to unity. Climate models and empirical evaluation from the climate change between the last ice age (Section 2.1 above) yield $g_{\text{fast feedbacks}}$ ~0.5-0.6 (the gain corresponding to fast feedback climate sensitivity 3°C for doubled CO_2). GHGs and surface albedo contribute about equally to glacial-interglacial 'forcings' and temperature change, with each having gain ~0.2 [14]. Thus

$$g = g_{\text{fast feedbacks}} + g_{\text{surface albedo}} + g_{\text{GHG}}$$
$$= \sim 0.5\text{-}0.6 + \sim 0.2 + \sim 0.2.$$

Thus climate gain in the Pleistocene was greater than or of the order of 0.9. It is no wonder that late Cenozoic climate fluctuated so greatly (Fig. **3b**). When substantial ice is present on the planet, g is close to unity, climate is sensitive, and large climate swings occur in response to small orbital forcings. Indeed, with g near unity any forcing or climate noise can cause large climate change, consistent with the conclusion that much of climate variability is not due to orbital forcings [S7]. In the early Cenozoic there was little ice, $g_{\text{surface albedo}}$ was small, and thus climate oscillations due to insolation perturbations were smaller.

It may be useful to divide inferences from Pleistocene climate change into two categories: (1) well-defined conclusions about the nature of the climate change, (2) less certain suggestions about the nature and causes of the climate change. The merit of identifying well-defined conclusions is that they help us predict likely consequences of human-made climate forcings. Less certain aspects of Pleistocene climate change mainly concern the small forcings that instigated climate swings. The small forcings are of great interest to paleoclimatologists, but they need not prevent extraction of practical implications from Pleistocene climate change.

Two fundamental characteristics of Pleistocene climate change are clear. First, there is the high gain, at least of the order of 0.9, i.e., the high sensitivity to a climate forcing, when the planet is in the range of climates that existed during the Pleistocene. Second, we have a good knowledge of the amplifying feedbacks that produce this high gain. Fast feedbacks, including water vapor, clouds, aerosols, sea ice and snow, contribute at least half of this gain. The remainder of the amplification is provided almost entirely by two factors: surface albedo (mainly ice sheets) and GHGs (mainly CO_2).

Details beyond these basic conclusions are less certain. The large glacial-interglacial surface albedo and GHG changes should lag global temperature, because they are feedbacks on global temperature on the global spatial scale and millennial time scale. The lag of GHGs after temperature change is several hundred years (Fig. **6** of [6]), perhaps determined by the ocean overturning time. Ice sheet changes may lag temperature by a few millennia [24], but it has been argued that there is no discernible lag between insolation forcing and the maximum rate of change of ice sheet volume [7].

A complication arises from the fact that some instigating factors (forcing mechanisms) for Pleistocene climate change also involve surface albedo and GHG changes. Regional anomalies of seasonal insolation are as much as many tens of W/m^2. The global forcing is small (Fig. **S3**) because the local anomalies are nearly balanced by anomalies of the opposite sign in either the opposite hemisphere or the opposite season. However, one can readily imagine climate change mechanisms that operate in such a way that cancellation does not occur.

For example, it has been argued [7] that a positive insolation anomaly in late spring is most effective for causing ice sheet disintegration because early 'albedo flip', as the ice becomes wet, yields maximum extension of the melt season. It is unlikely that the strong effect of albedo flip on absorbed solar energy could be offset by a negative insolation anomaly at other times of year.

A second example is non-cancellation of hemispheric insolation anomalies. A hemispheric asymmetry occurs when Earth is cold enough that ice sheets extend to Northern Hemisphere middle latitudes, due to absence of similar Southern Hemisphere land. It has been argued [7] that this hemispheric asymmetry is the reason that the orbital periodicities associated with precession of the equinoxes and orbit eccentricity became substantial about 1 million years ago.

Insolation anomalies also may directly affect GHG amounts, as well as surface albedo. One can readily imagine ways in which insolation anomalies affect methane release from wetlands or carbon uptake through biological processes.

Surface albedo and GHG changes that result immediately from insolation anomalies can be defined as climate forcings, as indirect forcings due to insolation anomalies. The question then becomes: what fractions of the known paleo albedo and GHG changes are immediate indirect forcings due to insolation anomalies and what fractions are feedbacks due to global temperature change?

It is our presumption that most of the Pleistocene GHG changes are a slow feedback in response to climate change. This interpretation is supported by the lag of several hundred years between temperature change and greenhouse gas amount (Fig. **6** of [6]). The conclusion that most of the ice area and surface albedo change is also a feedback in response to global temperature change is supported by the fact that the large climate swings are global (Section 5 of Appendix).

Note that our inferred climate sensitivity is not dependent on detailed workings of Pleistocene climate fluctuations. The fast feedback sensitivity of 3°C for doubled CO_2, derived by comparing glacial and interglacial states, is independent of the cause and dynamics of glacial/interglacial transitions.

Climate sensitivity including surface albedo feedback (~6°C for doubled CO_2) is the average sensitivity for the climate range from 35 My ago to the present and is independent of the glacial-interglacial 'wiggles' in Fig. (**3**). Note that climate and albedo changes occurred mainly at points with 'ready' [63] feedbacks: at Antarctic glaciation and (in the past three million years) with expansion of Northern Hemisphere glaciation, which are thus times of high climate sensitivity.

The entire ice albedo feedback from snowball-Earth to ice-free planet (or vice versa) can be viewed as a response to changing global temperature, with wiggles introduced by Milankovitch (orbital) forcings. The average $g_{surface\ albedo}$ for the range from today's climate through Antarctic deglaciation is close to $g_{surface\ albedo} \sim 0.2$, almost as large as in the Pleistocene. Beyond Antarctic deglaciation (i.e., for an ice-free planet) $g_{surface\ albedo} \rightarrow 0$, except for vegetation effects.

For the sake of specificity, let us estimate the effect of slow feedbacks on climate sensitivity. If we round ΔT_O to 1.2°C for doubled CO_2 and the fast feedback gain to $g_{fast\ feedbacks} = 0.6$, then for fast feedbacks alone f = 2.5 and the equilibrium warming is ΔT_{eq} = 3°C. Inclusion of $g_{surface\ albedo} = 0.2$ makes f = 5 and ΔT_{eq} = 6°C, which is the sensitivity if the GHG amount is specified from observations or from a carbon cycle model.

The feedback factor f can approach infinity, i.e., the climate can become unstable. However, instabilities are limited except at the snowball Earth and runaway greenhouse extremes. Some feedbacks have a finite supply, e.g., as when Antarctica becomes fully deglaciated. Also climate change can cause positive feedbacks to decrease or negative feedbacks to come into play.

For example, Fig. (**S2**) suggests that a cooling climate from the present state first reduces the fast feedback gain. This and reduced weathering with glaciation may be reasons that most ice ages did not reach closer to the iceball state. Also there may

be limitations on the ranges of GHG (CO_2, CH_4, N_2O) feedbacks. Empirical values g_{GHG} ~ 0.2 and $g_{surface\ albedo}$ ~ 0.2 were derived as averages relevant to the range of climates that existed in the past several hundred thousand years, and they may not be valid outside that range.

On the other hand, if the forcing becomes large enough, global instabilities are possible. Earth did become cold enough in the past for the snowball-Earth instability. Although the runaway greenhouse effect has not occurred on Earth, solar irradiance is now at its highest level so far, and Fig. (**S2**) suggests that the required forcing for runaway may be only 10-20 W/m^2. If all conventional and unconventional fossil fuels were burned, with the CO_2 emitted to the atmosphere, it is possible that a runaway greenhouse effect could occur, with incineration of life and creation of a permanent Venus-like hothouse Earth. It would take time for the ice sheets to melt, but the melt rate may accelerate as ice sheet disintegration proceeds.

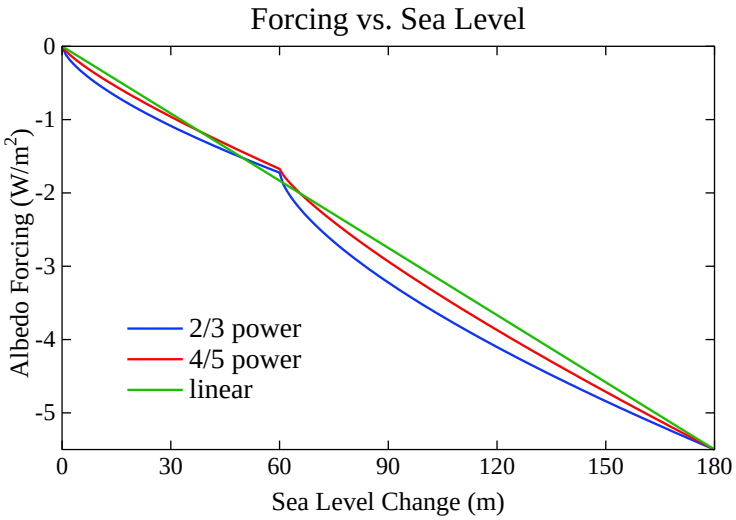

Fig. (S4). Surface albedo climate forcing as a function of sea level for three approximations of the ice sheet area as a function of sea level change, from an ice free planet to the last glacial maximum. For sea level between 0 and 60 m only Antarctica contributes to the albedo change. At the last glacial maximum Antarctica contains 75 m of sea level and the Northern Hemisphere contains 105 m.

4. ICE SHE*ET AL*BEDO

In the present paper we take the surface area covered by an ice sheet to be proportional to the 4/5 power of the volume of the ice sheet, based on ice sheet modeling of one of us (VM-D). We extend the formulation all the way to zero ice on the planet, with separate terms for each hemisphere. At 20 ky ago, when the ice sheets were at or near their maximum size in the Cenozoic era, the forcing by the Northern Hemisphere ice sheet was -3.5 W/m^2 and the forcing by the Southern Hemisphere ice sheet was -2 W/m^2, relative to the ice-free planet [14]. It is assumed that the first 60 m of sea level fall went entirely into growth of the Southern Hemisphere ice sheet. The water from further sea level fall is divided proportionately between hemispheres such that when sea level fall reaches -180 m there is 75 m in the ice sheet of the Southern Hemisphere and 105 m in the Northern Hemisphere.

The climate forcing due to sea level changes in the two hemispheres, SL_S and SL_N, is

$$F_{Albedo}\ (W/m^2) = -\ 2\ (SL_S/75\ m)^{4/5} - 3.5\ (SL_N/105\ m)^{4/5}, \qquad (S1)$$

where the climate forcings due to fully glaciated Antarctica (-2 W/m^2) and Northern Hemisphere glaciation during the last glacial maximum (-3.5 W/m^2) were derived from global climate model simulations [14].

Fig. (**S4**) compares results from the present approach with results from the same approach using exponent 2/3 rather than 4/5, and with a simple linear relationship between the total forcing and sea level change. Use of exponent 4/5 brings the results close to the linear case, suggesting that the simple linear relationship is a reasonably good approximation. The similarity of Fig. (**1c**) in our present paper and Fig. (**2c**) in [7] indicates that change of exponent from 2/3 to 4/5 did not have a large effect.

5. GLOBAL NATURE OF MAJOR CLIMATE CHANGES

Climate changes often begin in a specific hemisphere, but the large climate changes are invariably global, in part because of the global GHG feedback. Even without the GHG feedback, forcings that are located predominately in one hemisphere, such as ice sheet changes or human-made aerosols, still evoke a global response [12], albeit with the response being larger in the hemisphere of the forcing. Both the atmosphere and ocean transmit climate response between hemispheres. The deep ocean can carry a temperature change between hemispheres with little loss, but because of the ocean's thermal inertia there can be a hemispheric lag of up to a millennium (see Ocean Response Time, below).

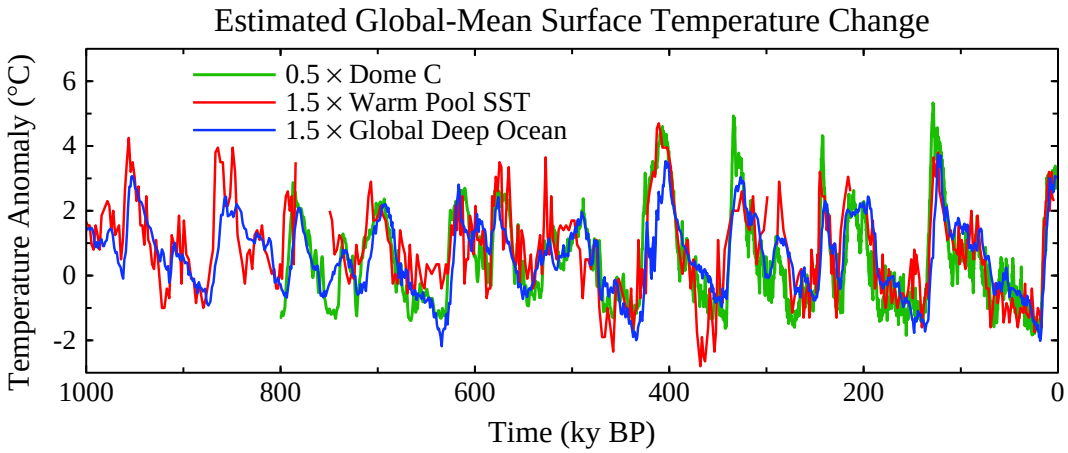

Fig. (S5). Estimated global temperature change based on measurements at a single point or, in the case of the deep ocean, a near-global stack of ocean drilling sites: Antarctica Dome C [S8], Warm Pool [S9], deep ocean [26].

Fig. (**S5**) compares temperature change in Antarctica [S8], the tropical sea surface [S9], and the global deep ocean [26]. Temperature records are multiplied by factors that convert the temperature record to an estimate of global temperature change. Based on paleoclimate records, polar temperature change is typically twice the global average temperature change, and tropical temperature change is about two-thirds of the global mean change. This polar amplification of the temperature change is an expected consequence of feedbacks [14], especially the snow-ice albedo feedback. The empirical result that deep ocean temperature changes are only about two-thirds as large as global temperature change is obtained from data for the Pleistocene epoch, when deep ocean temperature change is limited by its approach to the freezing point.

6. HOLOCENE CLIMATE FORCINGS

The GHG zero-point for the paleo portion of Fig. (**2**) is the mean for 10-8 ky BP, a time that should precede any significant anthropogenic effect on GHG amount. It has been suggested that the increase of CO_2 that began 8000 years ago is due to deforestation and the increase of CH_4 that began 6000 years ago is caused by rice agriculture [62]. This suggestion has proven to be controversial, but regardless of whether late Holocene CO_2 and CH_4 changes are human-made, the GHG forcing is anomalous in that period relative to global temperature change estimated from ocean and ice cores. As discussed elsewhere [7], the late Holocene is the only time in the ice core record in which there is a clear deviation of temperature from that expected due to GHG and surface albedo forcings.

The GHG forcing increase in the second half of the Holocene is ~3/4 W/m^2. Such a large forcing, by itself, would create a planetary energy imbalance that could not be sustained for millennia without causing a large global temperature increase, the expected global warming being about 1°C. Actual global temperature change in this period was small, perhaps a slight cooling. Fig. (**S6**) shows estimates of global temperature change obtained by dividing polar temperature change by two or multiplying tropical and deep ocean temperatures by 1.5. Clearly the Earth has not been warming rapidly in the latter half of the Holocene. Thus a substantial (negative) forcing must have been operating along with the positive GHG forcing.

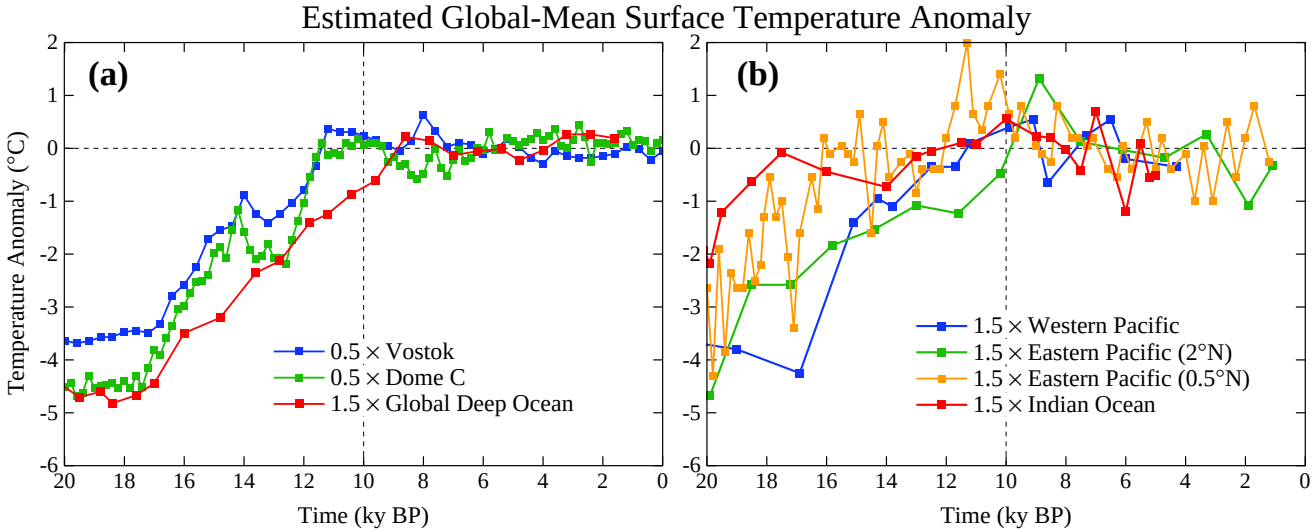

Fig. (S6). Estimates of global temperature change inferred from Antarctic ice cores [18, S8] and ocean sediment cores [S9-S13], as in Fig. (**S5**) but for a period allowing Holocene temperature to be apparent.

Deforestation causes a negative climate forcing [12], but an order of magnitude too small to balance GHG positive forcing. A much larger negative forcing is expected from human-made aerosols. Aerosol forcing is non-linear, especially the indirect effect on clouds, with aerosols added to a pristine atmosphere being more effective than those added to the current highly polluted atmosphere. Given estimates of a negative forcing of 1-2 W/m^2 for today's anthropogenic aerosols [2, 5, 12], a negative aerosol forcing at least of the order of 0.5 W/m^2 in 1850 is expected. We conclude that aerosols probably were the predominant negative forcing that opposed the rapid increase of positive GHG forcing in the late Holocene.

7. OCEAN RESPONSE TIME

Fig. (**S7**) shows the climate response function, defined as the fraction of equilibrium global warming that is obtained as a function of time. This response function was obtained [7] from a 3000-year simulation after instant doubling of atmospheric CO_2, using GISS modelE [S3, 12] coupled to the Russell ocean model [S14]. Note that although 40% of the equilibrium solution is obtained within several years, only 60% is achieved after a century, and nearly full response requires a millennium. The long response time is caused by slow uptake of heat by the deep ocean, which occurs primarily in the Southern Ocean.

This delay of the surface temperature response to a forcing, caused by ocean thermal inertia, is a strong (quadratic) function of climate sensitivity and it depends on the rate of mixing of water into the deep ocean [31]. The ocean model used for Fig. (**S7**) may mix somewhat too rapidly in the waters around Antarctica, as judged by transient tracers [S14], reducing the simulated surface response on the century time scale. However, this uncertainty does not qualitatively alter the shape of the response function (Fig. **S7**).

When the climate model used to produce Fig. (**S7**) is driven by observed changes of GHGs and other forcings it yields good agreement with observed global temperature and ocean heat storage [5]. The model has climate sensitivity ~3°C for doubled CO_2, in good agreement with the fast-feedback sensitivity inferred from paleoclimate data.

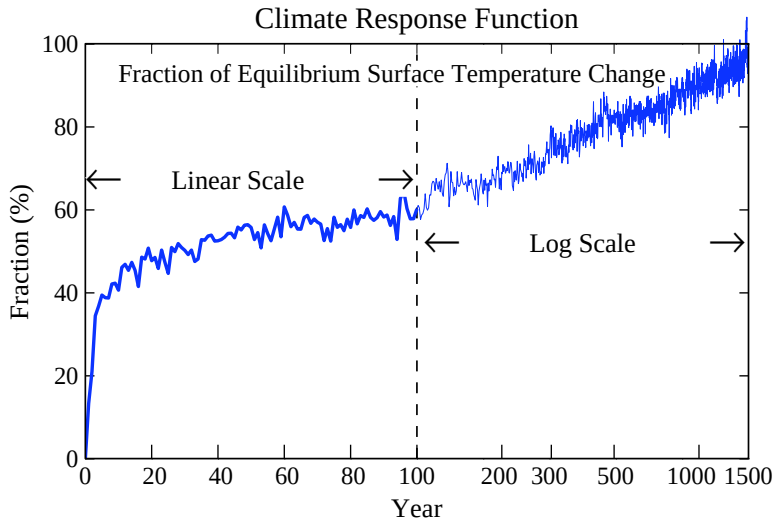

Fig. (S7). Fraction of equilibrium surface temperature response versus time in the GISS climate model [7, 12, S3] with the Russell [S14] ocean. The forcing was doubled atmospheric CO_2. The ice sheets, vegetation distribution and other long-lived GHGs were fixed.

8. SEPARATION OF $\Delta^{18}O$ INTO ICE VOLUME AND TEMPERATURE

$\delta^{18}O$ of benthic (deep ocean dwelling) foraminifera is affected by both deep ocean temperature and continental ice volume. Between 34 My and the last ice age (20 ky) the change of $\delta^{18}O$ was ~ 3, with T_{do} change ~ 6°C (from +5 to -1°C) and ice volume change ~ 180 msl (meters of sea level). Based on the rate of change of $\delta^{18}O$ with deep ocean temperature in the prior period without land ice, ~ 1.5 of $\delta^{18}O$ is associated with the T_{do} change of ~ 6°C, and we assign the remaining $\delta^{18}O$ change to ice volume linearly at the rate 60 msl per mil $\delta^{18}O$ change (thus 180 msl for $\delta^{18}O$ between 1.75 and 4.75).

Thus we assume that ice sheets were absent when $\delta^{18}O < 1.75$ with sea level 75 msl higher than today. Sea level at smaller values of $\delta^{18}O$ is given by

$$SL\ (m) = 75 - 60 \times (\delta^{18}O - 1.75). \qquad (S2)$$

Fig. (**S8**) shows that the division of $\delta^{18}O$ equally into sea level change and deep ocean temperature captures well the magnitude of the major glacial to interglacial changes.

9. CONTINENTAL DRIFT AND ATMOSPHERIC CO_2

At the beginning of the Cenozoic era 65 My ago the continents were already close to their present latitudes, so the effect of continental location on surface albedo had little direct effect on the planet's energy balance (Fig. **S9**). However, continental drift has a major effect on the balance, or imbalance, of outgassing and uptake of CO_2 by the solid Earth and thus a major effect on atmospheric composition and climate. We refer to the carbon in the air, ocean, soil and biosphere as the combined surface reservoir of carbon, and carbon in ocean sediments and the rest of the crust as the carbon in the 'solid' Earth. Sloshing of CO_2 among the surface reservoirs, as we have shown, is a primary mechanism for glacial-interglacial climate fluctuations. On longer time scales the total amount of carbon in the surface reservoirs can change as a result of any imbalance between outgassing and uptake by the solid Earth.

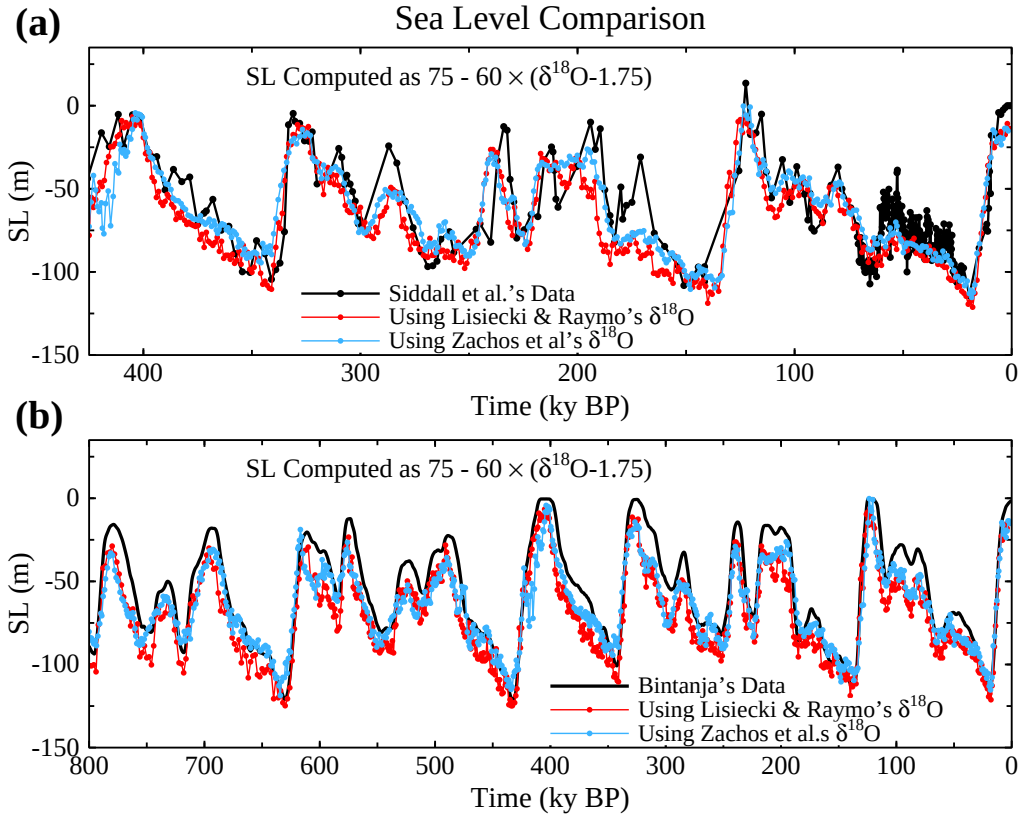

Fig. (S8). (**a**) Comparison of Siddall *et al.* [19] sea level record with sea level computed from $\delta^{18}O$ *via* Eq. S2 using two alternative global benthic stacks [26, S15]. (**b**) Comparison of Bintanja *et al.* [S16] sea level reconstruction with the same global benthic stacks as in (**a**).

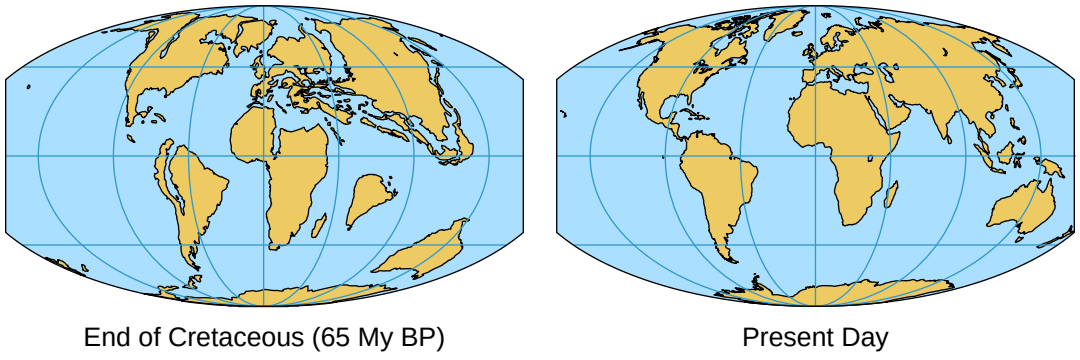

Fig. (S9). Continental locations at the beginning and end of the Cenozoic era [S17].

Outgassing, which occurs mainly in regions of volcanic activity, depends upon the rate at which carbon-rich oceanic crust is subducted beneath moving continental plates [30, 47]. Drawdown of CO_2 from the surface reservoir occurs with weathering of rocks exposed by uplift, with the weathering products carried by rivers to the ocean and eventually deposited as carbonates on the ocean floor [30] and by burial of organic matter. Both outgassing and drawdown of CO_2 are affected by changes in plate tectonics, which thus can alter the amount of carbon in the surface reservoir. The magnitude of the changes of carbon in the surface reservoir, and thus in the atmosphere, is constrained by a negative weathering feedback on the time scale of hundreds of thousands of years [30, 52], but plate tectonics can evoke changes of the surface carbon reservoir by altering the rates of outgassing and weathering.

At the beginning of the Cenozoic the African plate was already in collision with Eurasia, pushing up the Alps. India was still south of the equator, but moving north rapidly through a region with fresh carbonate deposits. It is likely that subduction of carbon rich crust of the Tethys Ocean, long a depocenter for sediments, caused an increase of atmospheric CO_2 and the early Cenozoic warming that peaked ~50 My ago. The period of rapid subduction terminated with the collision of India with Eurasia, whereupon uplift of the Himalayas and the Tibetan Plateau increased weathering rates and drawdown of atmospheric CO_2 [51].

Since 50 My ago the world's major rivers have emptied into the Indian and Atlantic Oceans, but there is little subduction of oceanic crust of these regions that are accumulating sediments [47]. Thus the collision of India with Asia was effective in both reducing a large source of outgassing of CO_2 as well as exposing rock for weathering and drawdown of atmospheric CO_2. The rate of CO_2 drawdown decreases as the CO_2 amount declines because of negative feedbacks, including the effects of temperature and plant growth rate on weathering [30].

10. PROXY CO_2 DATA

There are inconsistencies among the several proxy measures of atmospheric CO_2, including differences between results of investigators using nominally the same reconstruction method. We briefly describe strengths and weaknesses of the four paleo-CO_2 reconstruction methods included in the IPCC report [2], which are shown in Fig. (**S10**) and discussed in detail elsewhere [S18]. The inconsistencies among the different proxies constrain their utility for rigorously evaluating our CO_2 predictions. We also include a comparison of our calculated CO_2 history with results from a version of the Berner [30] geochemical carbon cycle model, as well as a comparison with an emerging CO_2 proxy based on carbon-isotope analyses of nonvascular plant (bryophyte) fossils [S19].

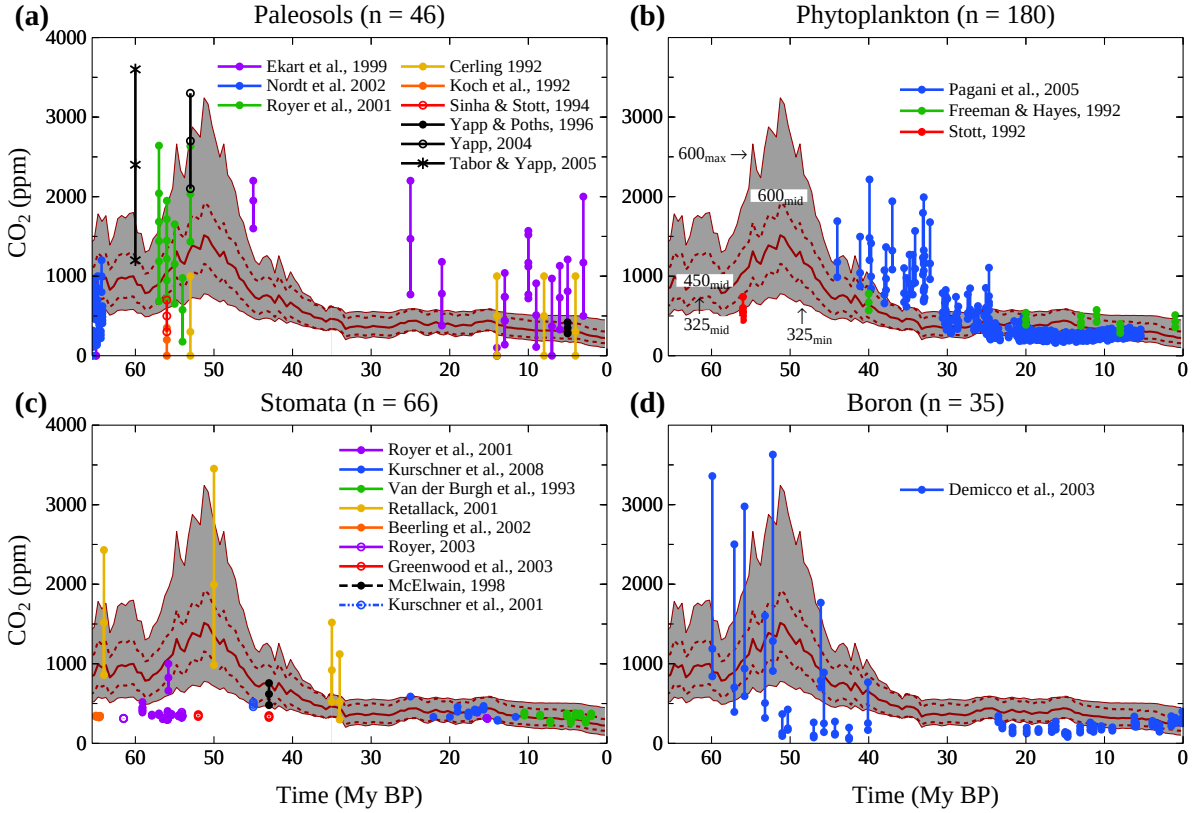

Fig. (S10). Comparison of proxy CO_2 measurements with CO_2 predictions based on deep-ocean temperature, the latter inferred from benthic $\delta^{18}O$. The shaded range of model results is intended mainly to guide the eye in comparing different proxies. The dark central line is for the standard case with CO_2 = 450 ppm at 35 My ago, and the dashed lines are the standard cases for CO_2 = 325 and 600 ppm at 35 My ago. The extremes of the shaded area correspond to the maximum range including a 50% uncertainty in the relation of ΔT_s and ΔT_{do}. Our assumption that CO_2 provides 75% of the GHG throughout the Cenozoic adds additional uncertainty to the predicted CO_2 amount. References for data sources in the legends are provided by Royer [55], except Kurshner *et al.* [S20].

The paleosol method is based on the $\delta^{13}C$ of pedogenic carbonate nodules, whose formation can be represented by a two end-member mixing model between atmospheric CO_2 and soil-derived carbon [S21]. Variables that need to be constrained or assumed include an estimation of nodule depth from the surface of the original soil, the respiration rate of the ecosystem that inhabits the soil, the porosity/diffusivity of the original soil, and the isotopic composition of the vegetation contribution of respired CO_2. The uncertainties in CO_2 estimates with this proxy are substantial at high CO_2 (±500-1000 ppm when CO_2 > 1000 ppm) and somewhat less in the lower CO_2 range (±400-500 ppm when CO_2 < 1000 ppm).

The stomatal method is based on the genetically-controlled relationship [S22] between the proportion of leaf surface cells that are stomata and atmospheric CO_2 concentrations [S23]. The error terms with this method are comparatively small at low CO_2 (< ±50 ppm), but the method rapidly loses sensitivity at high CO_2 (> 500-1000 ppm). Because stomatal-CO_2 relationships are often species-specific, only extant taxa with long fossil records can be used [S24]. Also, because the fundamental response of stomata is to the partial pressure of CO_2 [S25], constraints on paleoelevation are required.

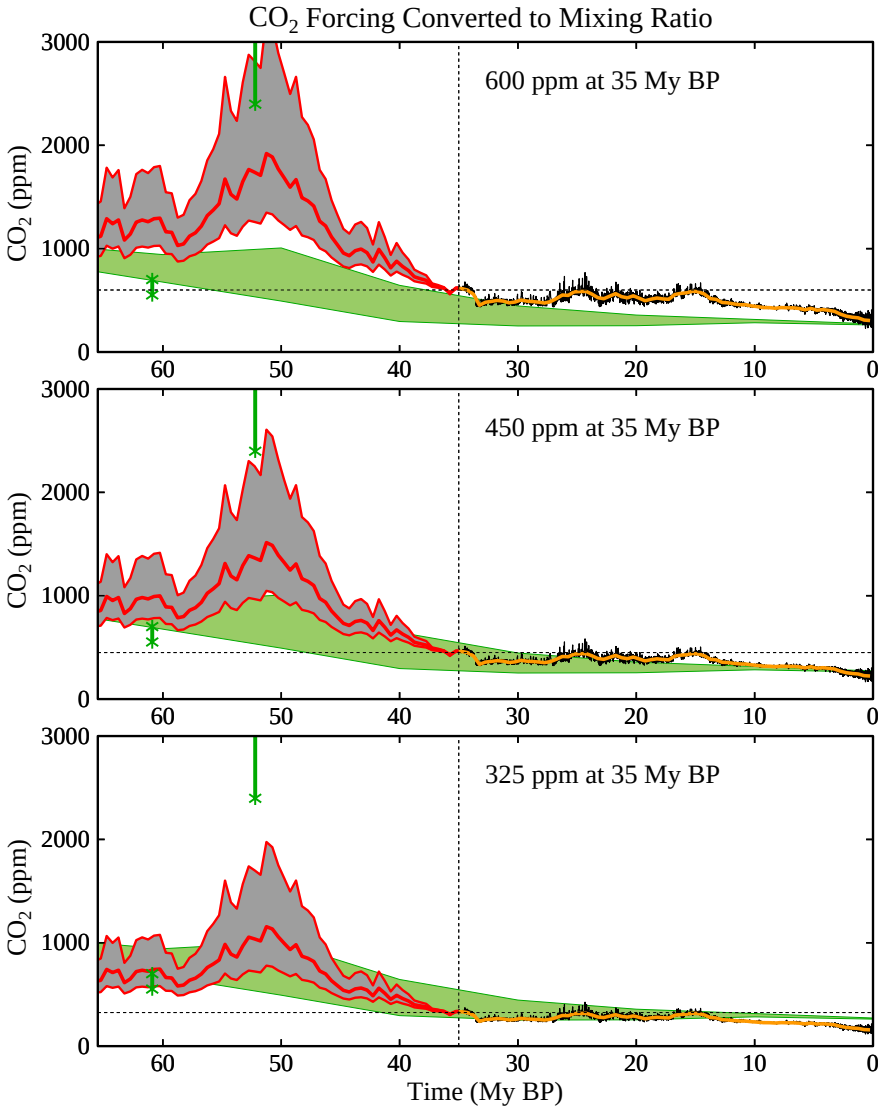

Fig. (S11). Simulated CO_2 in the Cenozoic for three choices of CO_2 amount at 35 My, as in Fig. (**5**), compared with the CO_2 history in a geochemical model [30], specifically the model version described by Fletcher *et al.* [S19]. The green vertical bars are a proxy CO_2 measure [S19] obtained from fossils of non-vascular plants (bryophytes) that is not included among the proxies shown in Fig. (**S10**).

The phytoplankton method is based on the Rayleigh distillation process of fractionating stable carbon isotopes during photosynthesis [S26]. In a high CO_2 environment, for example, there is a higher diffusion rate of CO_2 through phytoplankton cell membranes, leading to a larger available intercellular pool of $CO_{2[aq]}$ and more depleted $\delta^{13}C$ values in photosynthate. Cellular growth rate and cell size also impact the fractionation of carbon isotopes in phytoplankton and thus fossil studies must take these factors into account [S27]. This approach to reconstructing CO_2 assumes that the diffusional transport of CO_2 into the cell dominates, and that any portion of carbon actively transported into the cell remains constant with time. Error terms are typically small at low CO_2 (< ±50 ppm) and increase substantially under higher CO_2 concentrations [S27].

The boron-isotope approach is based on the pH-dependency of the $\delta^{11}B$ of marine carbonate [S28]. This current method assumes that only borate is incorporated in the carbonate lattice and that the fractionation factor for isotope exchange between boric acid and borate in solution is well-constrained. Additional factors that must be taken into account include test dissolution and size, species-specific physiological effects on carbonate $\delta^{11}B$, and ocean alkalinity [S29-S31]. As with the stomatal and phytoplankton methods, error terms are comparatively small at low CO_2 (< ±50 ppm) and the method loses sensitivity at higher CO_2 (> 1000 ppm). Uncertainty is unconstrained for extinct foraminiferal species.

Fig. (**S10**) illustrates the scatter among proxy data sources, which limits inferences about atmospheric CO_2 history. Given the large inconsistency among different data sets in the early Cenozoic, at least some of the data or their interpretations must be flawed. In the range of proxy data shown in Fig. (**5**) we took all data sources as being of equal significance. It seems likely that the low CO_2 values in the early Cenozoic are faulty, but we avoid omission of any data until the matter is clarified, and thus the range of proxy data shown in Fig. (**5**) is based on all data. Reviews of the proxy data [S19, 55] conclude that atmospheric CO_2 amount in the early Cenozoic reached values of at least 500-1000 ppm.

Fig. (**S11**) shows that geochemical carbon cycle modeling [30, S19] is reasonably consistent with our calculated long-term trend of atmospheric CO_2 for the cases with CO_2 at 34 My ago being in the range from about 325 to 450 ppm. The geochemical modeling does not yield a strong maximum of CO_2 at 50 My ago, but the temporal resolution of the modeling (10 My) and the absence of high resolution input data for outgassing due to variations in plate motions tends to mitigate against sharp features in the simulated CO_2.

Fig. (**S11**) also shows (vertical green bars) an emerging CO_2 proxy based on the isotopic composition of fossil liverworts. These non-vascular plants, lacking stomatal pores, have a carbon isotopic fractionation that is strongly CO_2 dependent, reflecting the balance between CO_2 uptake by photosynthesis and inward CO_2 diffusion [S19].

11. CLIMATE SENSITIVITY COMPARISONS

Other empirical or semi-empirical derivations of climate sensitivity from paleoclimate data (Table **S1**) are in reasonable accord with our results, when account is taken of differences in definitions of sensitivity and the periods considered.

Royer *et al*. [56] use a carbon cycle model, including temperature dependence of weathering rates, to find a best-fit doubled CO_2 sensitivity of 2.8°C based on comparison with Phanerozoic CO_2 proxy amounts. Best-fit in their comparison of model and proxy CO_2 data is dominated by the times of large CO_2 in the Phanerozoic, when ice sheets would be absent, not by the times of small CO_2 in the late Cenozoic. Their inferred sensitivity is consistent with our inference of ~3°C for doubled CO_2 at times of little or no ice on the planet.

Higgins and Schrag [57] infer climate sensitivity of ~4°C for doubled CO_2 from the temperature change during the Paleocene-Eocene Thermal Maximum (PETM) ~55 My ago (Fig. **3**), based on the magnitude of the carbon isotope excursion at that time. Their climate sensitivity for an ice-free planet is consistent with ours within uncertainty ranges. Furthermore, recalling that we assume non-CO_2 to provide 25% of the GHG forcing, if one assumes that part of the PETM warming was a direct of effect of methane, then their inferred climate sensitivity is in even closer agreement with ours.

Pagani *et al.* [58] also use the magnitude of the PETM warming and the associated carbon isotopic excursion to discuss implications for climate sensitivity, providing a graphical relationship to help assess alternative assumptions about the origin and magnitude of carbon release. They conclude that the observed PETM warming of about 5°C implies a high climate sensitivity, but with large uncertainty due to imprecise knowledge of the carbon release.

Table S1. Climate Sensitivity Inferred Semi-Empirically from Cenozoic or Phanerozoic Climate Change

Reference	Period	Doubled CO_2 Sensitivity
Royer *et al.* [56]	0-420 My	~ 2.8°C
Higgins and Schrag [57]	PETM	~4°C
Pagani *et al.* [58]	PETM	High

12. GREENHOUSE GAS GROWTH RATES

Fossil fuel CO_2 emissions have been increasing at a rate close to the highest IPCC [S34] scenario (Fig. **S12b**). Increase of CO_2 in the air, however, appears to be in the middle of the IPCC scenarios (Fig. **S12c**, **d**), but as yet the scenarios are too close and interannual variability too large, for assessment. CO_2 growth is well above the "alternative scenario", which was defined with the objective of keeping added GHG forcing in the 21st century at about 1.5 W/m^2 and 21st century global warming less than 1°C [20].

Non-CO_2 greenhouse gases are increasing more slowly than in IPCC scenarios, overall at approximately the rate of the "alternative scenario", based on a review of data through the end of 2007 [69]. There is potential to reduce non-CO_2 forcings below the alternative scenario [69].

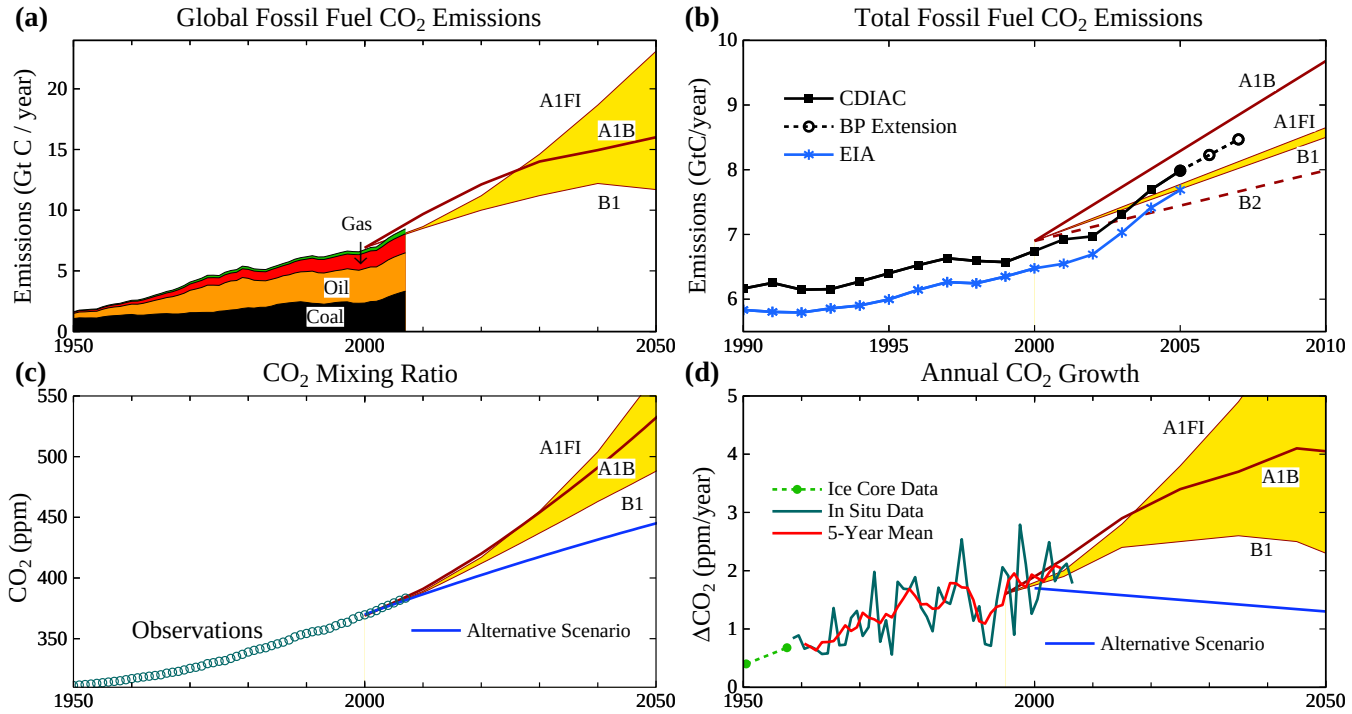

Fig. (S12). (**a**) Fossil fuel CO_2 emissions by fuel type [S32, S33], the thin green sliver being gas flaring plus cement production, and IPCC fossil fuel emissions scenarios, (**b**) expansion global emissions to show recent changes more precisely, the EIA values excluding CO_2 emissions from cement manufacture, (**c**) observed atmospheric CO_2 amount and IPCC and "alternative" scenarios for the future, (**d**) annual atmospheric CO_2 growth rates. Data here is an update of data sources defined in [6]. The yellow area is bounded by scenarios that are most extreme in the second half of the 21st century; other scenarios fall outside this range in the early part of the century.

13. FOSSIL FUEL AND LAND-USE CO_2 EMISSIONS

Fig. (**S13**) shows estimates of anthropogenic CO_2 emissions to the atmosphere. Although fossil emissions through 2006 are known with good accuracy, probably better than 10%, reserves and potential reserve growth are highly uncertain. IPCC [S34] estimates for oil and gas proven reserves are probably a lower limit for future oil and gas emissions, but they are perhaps a feasible goal that could be achieved *via* a substantial growing carbon price that discourages fossil fuel exploration in extreme environments together with national and international policies that accelerate transition to carbon-free energy sources and limit fossil fuel extraction in extreme environments and on government controlled property.

Coal reserves are highly uncertain, but the reserves are surely enough to take atmospheric CO_2 amount far into the region that we assess as being "dangerous". Thus we only consider scenarios in which coal use is phased out as rapidly as possible, except for uses in which the CO_2 is captured and stored so that it cannot escape to the atmosphere. Thus the magnitude of coal reserves does not appreciably affect our simulations of future atmospheric CO_2 amount.

Integrated 1850-2008 net land-use emissions based on the full Houghton [83] historical emissions (Fig. **S14**), extended with constant emissions for the past several years, are 79 ppm CO_2. Although this could be an overestimate by up to a factor of two (see below), substantial pre-1850 deforestation must be added in. Our subjective estimate of uncertainty in the total land-use CO_2 emission is a factor of two.

14. THE MODERN CARBON CYCLE

Atmospheric CO_2 amount is affected significantly not only by fossil fuel emissions, but also by agricultural and forestry practices. Quantification of the role of land-use in the uptake and release of CO_2 is needed to assess strategies to minimize human-made climate effects.

Fig. (**S15**) shows the CO_2 airborne fraction, AF, the annual increase of atmospheric CO_2 divided by annual fossil fuel CO_2 emissions. AF is a critical metric of the modern carbon cycle, because it is based on the two numbers characterizing the global carbon cycle that are well known. AF averages 56% over the period of accurate data, which began with the CO_2 measurements of Keeling in 1957, with no discernable trend. The fact that 44% of fossil fuel emissions seemingly "disappears" immediately provides a hint of optimism with regard to the possibility of stabilizing, or reducing, atmospheric CO_2 amount.

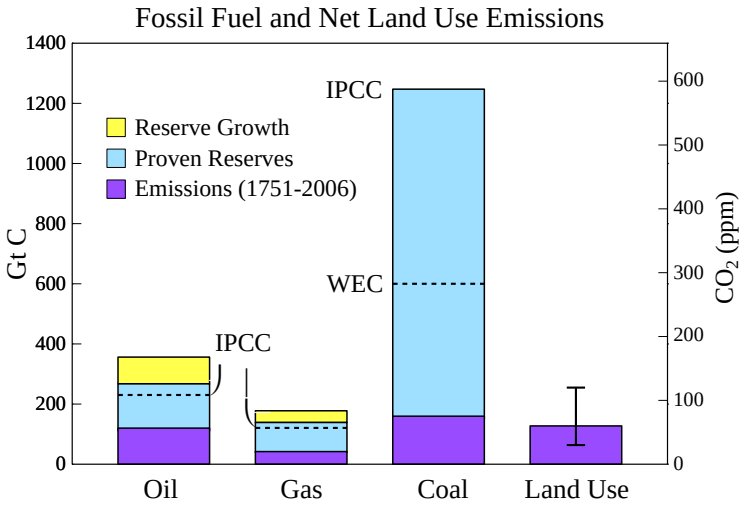

Fig. (S13). Fossil fuel and land-use CO_2 emissions, and potential fossil fuel emissions. Historical fossil fuel emissions are from the Carbon Dioxide Information Analysis Center [CDIAC, S32] and British Petroleum [BP, S33]. Lower limits on oil and gas reserves are from IPCC [S34] and higher limits are from the United States Energy Information Administration [EIA, 80]. Lower limit for coal reserves is from the World Energy Council [WEC, S35] and upper limit from IPCC [S34]. Land use estimate is from integrated emissions of Houghton/2 (Fig. **S14**) supplemented to include pre-1850 and post-2000 emissions; uncertainty bar is subjective.

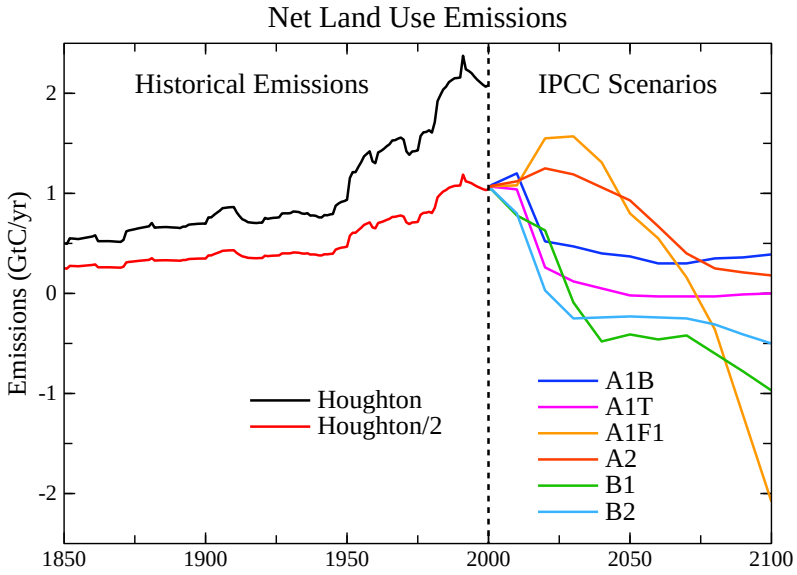

Fig. (S14). Left side: estimate by Houghton [83] of historical net land-use CO_2 emissions, and a 50 percent reduction of that estimate. Right side: IPCC [2] scenarios for land-use CO_2 emissions.

That optimism needs to be tempered, as we will see, by realization of the magnitude of the actions required to halt and reverse CO_2 growth. However, it is equally important to realize that assertions that fossil fuel emissions must be reduced close to 100% on an implausibly fast schedule are not necessarily valid.

A second definition of the airborne fraction, AF2, is also useful. AF2 includes the net anthropogenic land-use emission of CO_2 in the denominator. This AF2 definition of airborne fraction has become common in recent carbon cycle literature. However, AF2 is not an observed or accurately known quantity; it involves estimates of net land-use CO_2 emissions, which vary among investigators by a factor of two or more [2].

Fig. (**S15**) shows an estimate of net land-use CO_2 emissions commonly used in carbon cycle studies, labeled "Houghton" [83], as well as "Houghton/2", a 50% reduction of these land-use emissions. An over-estimate of land-use emissions is one possible solution of the long-standing "missing sink" problem that emerges when the full "Houghton" land-use emissions are employed in carbon cycle models [2, S34, 79].

Principal competing solutions of the "missing sink" paradox are (1) land-use CO_2 emissions are over-estimated by about a factor of two, or (2) the biosphere is being "fertilized" by anthropogenic emissions, *via* some combination of increasing atmospheric CO_2, nitrogen deposition, and global warming, to a greater degree than included in typical carbon cycle models.

Reality may include contributions from both candidate explanations. There is also a possibility that imprecision in the ocean uptake of CO_2, or existence of other sinks such as clay formation, could contribute increased CO_2 uptake, but these uncertainties are believed to be small.

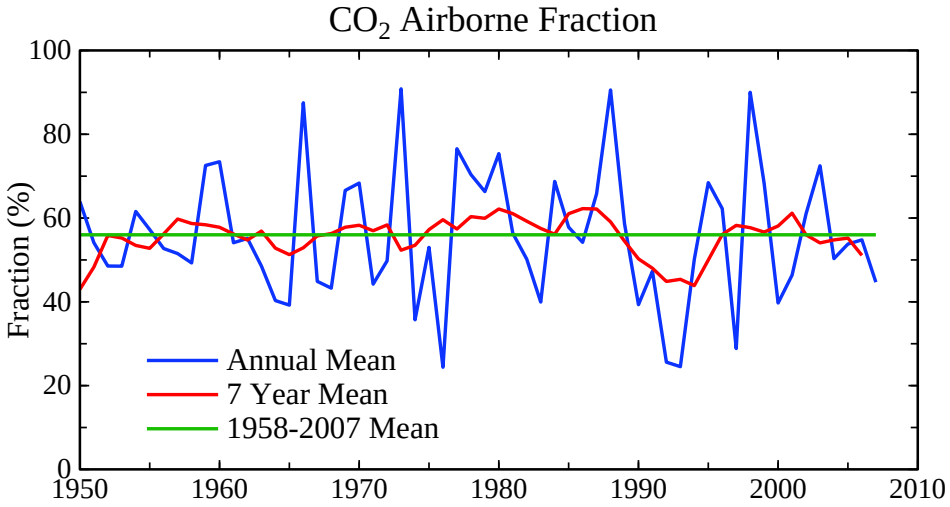

Fig. (S15). CO_2 airborne fraction, AF, the ratio of annual observed atmospheric CO_2 increase to annual fossil fuel CO_2 emissions.

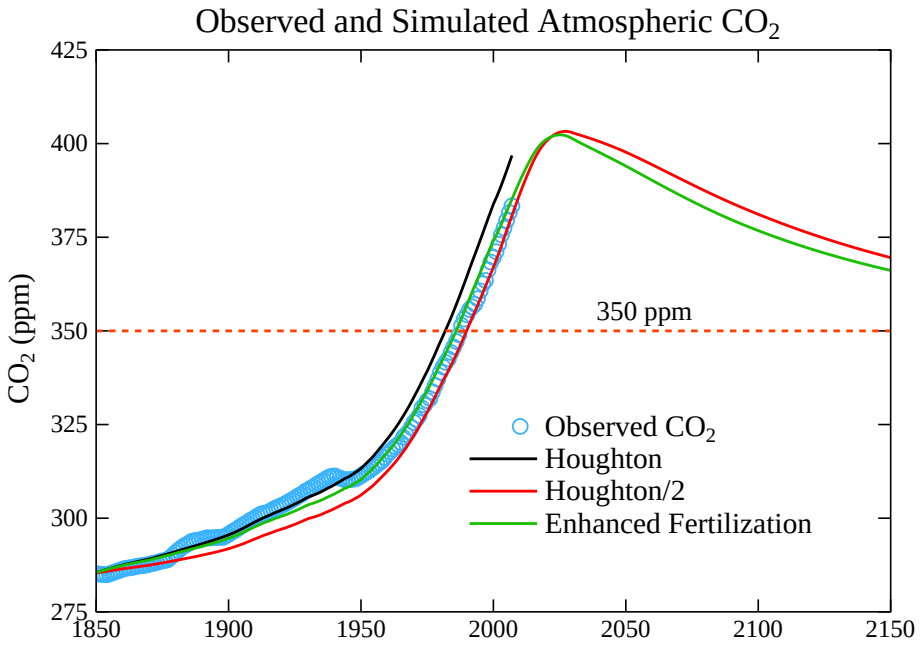

Fig. (S16). Computed and observed time evolution of atmospheric CO_2. "Enhanced Fertilization" uses the full "Houghton" land use emissions for 1850–2000. "Houghton/2" and "Enhanced Fertilization" simulations are extended to 2100 assuming coal phase-out by 2030 and the IPCC [2] A1T land-use scenario. Observations are from Law Dome ice core data and flask and in-situ measurements [6, S36, http://www.esrl.noaa.gov/gmd/ccgg/trends/].

Fig. (**S16**) shows resulting atmospheric CO_2, and Fig. (**S17**) shows AF and AF2, for two extreme assumptions: "Houghton/2" and " Enhanced Fertilization", as computed with a dynamic-sink pulse response function (PRF) representation of the Bern carbon cycle model [78, 79]. Fertilization is implemented *via* a parameterization [78] that can be adjusted to achieve an improved match between observed and simulated CO_2 amount. In the "Houghton/2" simulation the original value [78] of the fertilization parameter is employed while in the "Enhanced Fertilization" simulation the full Houghton emissions are used with a larger fertilization parameter. Both "Houghton/2" and "Enhanced Fertilization" yield good agreement with the observed CO_2 history, but Houghton/2 does a better job of matching the time dependence of observed AF.

It would be possible to match observed CO_2 to an arbitrary precision if we allowed the adjustment to "Houghton" land-use to vary with time, but there is little point or need for that. Fig. (**S16**) shows that projections of future CO_2 do not differ much even for the extremes of Houghton/2 and Enhanced Fertilization. Thus in Fig. (**6**) we show results for only the case Houghton/2, which is in better agreement with the airborne fraction and also is continuous with IPCC scenarios for land use.

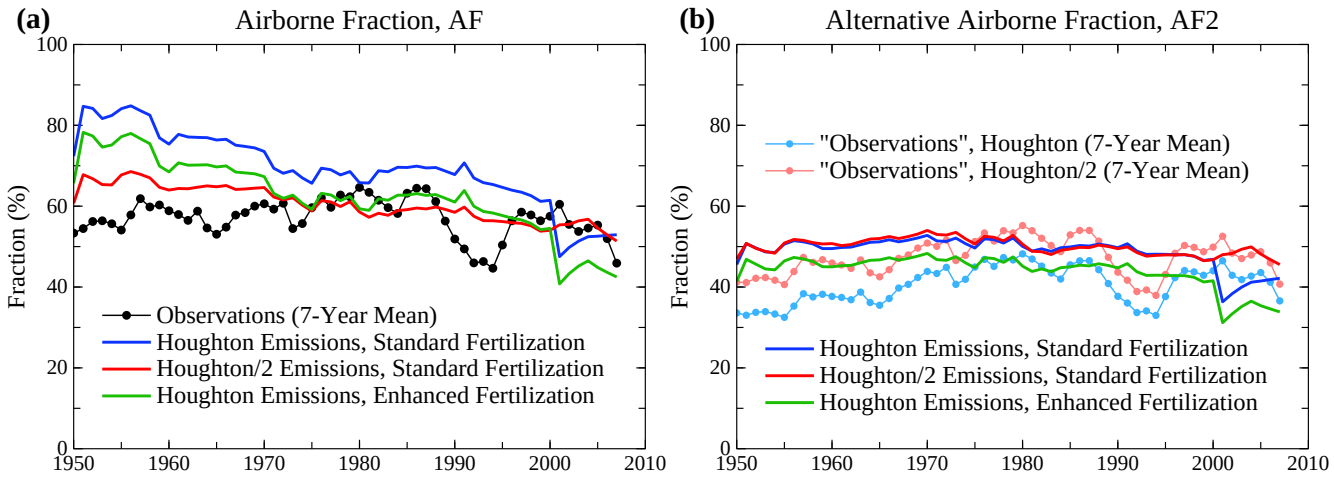

Fig. (S17). (**a**) Observed and simulated airborne fraction (AF), the ratio of annual CO_2 increase in the air over annual fossil fuel CO_2 emissions, (**b**) AF2 includes the sum of land use and fossil fuel emissions in the denominator in defining airborne fraction; thus AF2 is not accurately known because of the large uncertainty in land use emissions.

15. IMPLICATIONS OF FIG. (6): CO_2 EMISSIONS AND ATMOSPHERIC CONCENTRATION WITH COAL PHASE-OUT BY 2030

Fig. (**6**) provides an indication of the magnitude of actions that are needed to return atmospheric CO_2 to a level of 350 ppm or lower. Fig. (**6**) allows for the fact that there is disagreement about the magnitude of fossil fuel reserves, and that the magnitude of useable reserves depends upon policies.

A basic assumption underlying Fig. (**6**) is that, within the next several years, there will be a moratorium on construction of coal-fired power plants that do not capture and store CO_2, and that CO_2 emissions from existing power plants will be phased out by 2030. This coal emissions phase out is the sine qua non for stabilizing and reducing atmospheric CO_2. If the sine qua non of coal emissions phase-out is achieved, atmospheric CO_2 can be kept to a peak amount ~400-425 ppm, depending upon the magnitude of oil and gas reserves.

Fig. (**6**) illustrates two widely different assumptions about the magnitude of oil and gas reserves (illustrated in Fig. **S13**). The smaller oil and gas reserves, those labeled “IPCC”, are realistic if “peak oil” advocates are more-or-less right, i.e., if the world has already exploited about half of readily accessible oil and gas deposits, so that production of oil and gas will begin to decline within the next several years.

There are also “resource optimists” who dispute the “peakists’, arguing that there is much more oil (and gas) to be found. It is possible that both the “peakists” and “resource optimists” are right, it being a matter of how hard we work to extract maximum fossil fuel resources. From the standpoint of controlling human-made climate change, it does not matter much which of these parties is closer to the truth.

Fig. (**6**) shows that, if peak CO_2 is to be kept close to 400 ppm, the oil and gas reserves actually exploited need to be close to the “IPCC” reserve values. In other words, if we phase out coal emissions we can use remaining oil and gas amounts equal to those which have already been used, and still keep peak CO_2 at about 400 ppm. Such a limit is probably necessary if we are to retain the possibility of a drawdown of CO_2 beneath the 350 ppm level by methods that are more-or-less “natural”. If, on the other hand, reserve growth of the magnitude that EIA estimates (Figs. **6** and **S13**) occurs, and if these reserves are burned with the CO_2 emitted to the atmosphere, then the forest and soil sequestration that we discuss would be inadequate to achieve drawdown below the 350 ppm level in less than several centuries.

Even if the greater resources estimated by EIA are potentially available, it does not mean that the world necessarily must follow the course implied by EIA estimates for reserve growth. If a sufficient price is applied to carbon emissions it will discourage extraction of fossil fuels in the most extreme environments. Other actions that would help keep effective reserves close to the IPCC estimates would include prohibition of drilling in environmentally sensitive areas, including the Arctic and Antarctic.

National policies, in most countries, have generally pushed to expand fossil fuel reserves as much as possible. This might partially account for the fact that energy information agencies, such as the EIA in the United States, which are government agencies, tend to forecast strong growth of fossil fuel reserves. On the other hand, state, local, and citizen organizations can influence imposition of limits on fossil fuel extraction, so there is no guarantee that fossil resources will be fully exploited. Once the successors to fossil energy begin to take hold, there may be a shifting away from fossil fuels that leaves some of the resources in the ground. Thus a scenario with oil and gas emissions similar to that for IPCC reserves may be plausible.

Assumptions yielding the Forestry & Soil wedge in Fig. (**6b**) are as follows. It is assumed that current net deforestation will decline linearly to zero between 2010 and 2015. It is assumed that uptake of carbon *via* reforestation will increase linearly until 2030, by which time reforestation will achieve a maximum potential sequestration rate of 1.6 GtC per year [S37]. Waste-derived biochar application will be phased in linearly over the period 2010-2020, by which time it will reach a maximum uptake rate of 0.16 GtC/yr [85]. Thus after 2030 there will be an annual uptake of 1.6 + 0.16 = 1.76 GtC per year, based on the two processes described.

Thus Fig. (**6**) shows that the combination of (1) moratorium and phase-out of coal emissions by 2030, (2) policies that effectively keep fossil fuel reserves from significantly exceeding the IPCC reserve estimates, and (3) major programs to achieve carbon sequestration in forests and soil, can together return atmospheric CO_2 below the 350 ppm level before the end of the century.

The final wedge in Fig. (**6**) is designed to provide an indication of the degree of actions that would be required to bring atmospheric CO_2 back to the level of 350 ppm by a time close to the middle of this century, rather than the end of the century. This case also provides an indication of how difficult it would be to compensate for excessive coal emissions, if the world should fail to achieve a moratorium and phase-out of coal as assumed as our "sine qua non".

Assumptions yielding the Oil-Gas-Biofuels wedge in Fig. (**6b**) are as follows: energy efficiency, conservation, carbon pricing, renewable energies, nuclear power and other carbon-free energy sources, and government standards and regulations will lead to decline of oil and gas emissions at 4% per year beginning when 50% of the estimated resource (oil or gas) has been exploited, rather than the 2% per year baseline decline rate [79]. Also capture of CO_2 at gas- power plants (with CO_2 capture) will use 50% of remaining gas supplies. Also a linear phase-in of liquid biofuels is assumed between 2015 and 2025 leading to a maximum global bioenergy from "low-input/high-diversity" biofuels of ~23 EJ/yr, inferred from Tilman *et al*. [87], that is used as a substitute for oil; this is equivalent to ~0.5 GtC/yr, based on energy conversion of 50 EJ/GtC for oil. Finally, from 2025 onward, twice this number (i.e., 1 GtC/yr) is subtracted from annual oil emissions, assuming root/soil carbon sequestration *via* this biofuel-for-oil substitution is at least as substantial as in Tilman *et al.* [87]. An additional option that could contribute to this wedge is using biofuels in powerplants with CO_2 capture and sequestration [86].

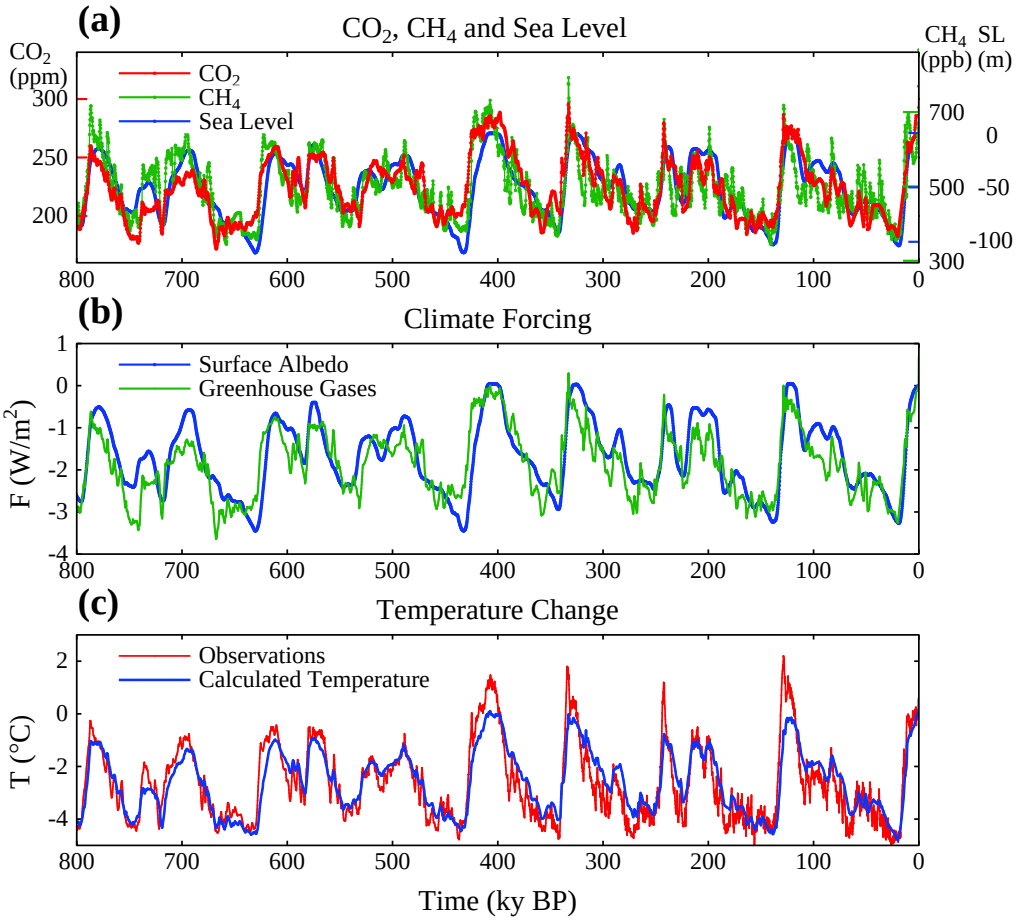

Fig. (S18). (**a**) CO_2 [S38], CH_4 [S39] and sea level [S16] for past 800 ky. (**b**) Climate forcings due to changes of GHGs and ice sheet area, the latter inferred from the sea level history of Bintanja *et al.* [S16]. (**c**) Calculated global temperature change based on the above forcings and climate sensitivity ¾°C per W/m^2. Observations are Antarctic temperature change from the Dome C ice core [S8] divided by two.

16. EPICA 800 KY DATA

Antarctic Dme C ice core data acquired by EPICA (European Project for Ice Coring in Antarctica) provide a record of atmospheric composition and temperature spanning 800 ky [S8], almost double the time covered by the Vostok data [17, 18] of Figs. (**1**) and (**2**). This extended record allows us to examine the relationship of climate forcing mechanisms and temperature change over a period that includes a substantial change in the nature of glacial-interglacial climate swings. During the first half of the EPICA record, the period 800-400 ky BP, the climate swings were smaller, sea level did not rise as high as the present level, and the GHGs did not increase to amounts as high as those of recent interglacial periods.

Fig. (**S18**) shows that the temperature change calculated exactly as described for the Vostok data of Fig. (**1**), i.e., multiplying the fast-feedback climate sensitivity ¾°C per W/m^2 by the sum of the GHG and surface albedo forcings (Fig. **S18b**), yields a remarkably close fit in the first half of the Dome C record to one-half of the temperature inferred from the isotopic composition of the ice. In the more recent half of the record slightly larger than ¾°C per W/m^2 would yield a noticeably better fit to the observed Dome C temperature divided by two (Fig. **S19**). However, there is no good reason to change our approximate estimate of ¾°C per W/m^2, because the assumed polar amplification by a factor of two is only approximate.

The sharper spikes in recent observed interglacial temperature, relative to the calculated temperature, must be in part an artifact of differing temporal resolutions. Temperature is inferred from the isotopic composition of the ice, being a function of the temperature at which the snowflakes formed, and thus inherently has a very high temporal resolution. GHG amounts, in contrast, are smoothed over a few ky by mixing of air in the snow that occurs up until the snow is deep enough for the snow to be compressed into ice. In the central Antarctic, where both Vostok and Dome C are located, bubble closure requires a few thousand years [17].

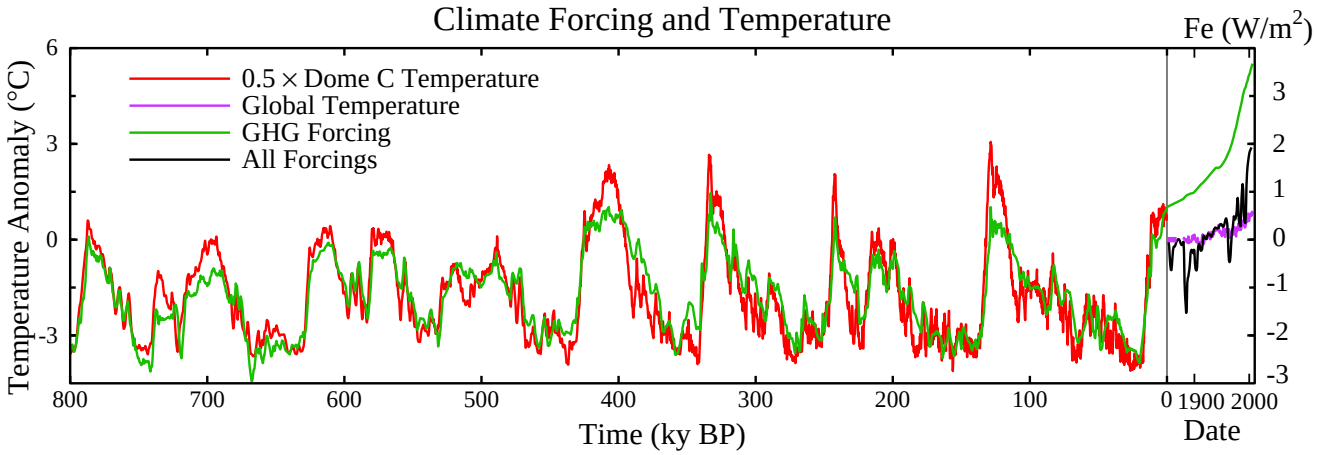

Fig. (S19). Global temperature change (left scale) estimated as half of temperature change from Dome C ice core [S8] and GHG forcing (right scale) due to CO_2, CH_4 and N_2O [S38, S39]. Ratio of temperature and forcing scales is 1.5°C per W/m^2. Time scale is expanded in the extension to recent years. Modern forcings include human-made aerosols, volcanic aerosols and solar irradiance [5]. GHG forcing zero point is the mean for 10-8 ky before present. Net climate forcing and modern temperature zero points are at 1850. The implicit presumption that the positive GHG forcing at 1850 is largely offset by negative human-made forcings [7] is supported by the lack of rapid global temperature change in the Holocene (Fig. **S6**).

17. COMPARISON OF ANTARCTIC DATA SETS

Fig. (**S20**) compares Antarctic data sets used in this supplementary section and in our parent paper. This comparison is also relevant to interpretations of the ice core data in prior papers using the original Vostok data.

The temperature records of Petit *et al.* [17] and Vimeux *et al.* [18] are from the same Vostok ice core, but Vimeux *et al.* [18] have adjusted the temperatures with a procedure designed to correct for climate variations in the water vapor source regions. The isotopic composition of the ice is affected by the climate conditions in the water vapor source region as well as by the temperature in the air above Vostok where the snowflakes formed; thus the adjustment is intended to yield a record that more accurately reflects the air temperature at Vostok. The green temperature curve in Fig. (**S20c**), which includes the adjustment, reduces the amplitude of glacial-interglacial temperature swings from those in the original (red curve) Petit *et al.* [17] data. Thus it seems likely that there will be some reduction of the amplitude and spikiness of the Dome C temperature record when a similar adjustment is made to the Dome C data set.

The temporal shift of the Dome C temperature data [S8], relative to the Vostok records, is a result of the improved EDC3 [S40, S41] time scale. With this new time scale, which has a 1σ uncertainty of ~3 ky for times earlier than ~130 ky BP, the rapid temperature increases of Termination IV (~335 ky BP) and Termination III (~245 ky BP) are in close agreement with the contention [7] that rapid ice sheet disintegration and global temperature rise should be nearly simultaneous with late spring

(April-May-June) insolation maxima at 60N latitude, as was already the case for Terminations II and I, whose timings are not significantly affected by the improved time scale.

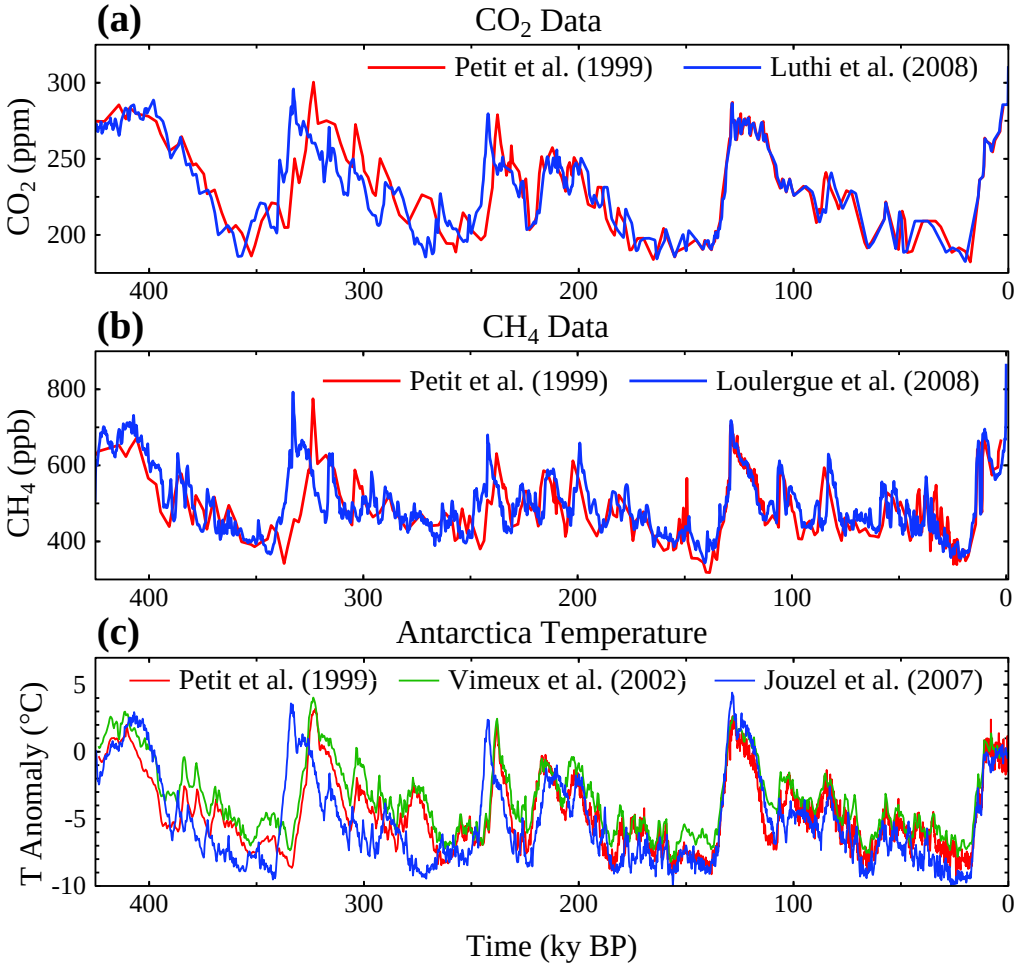

Fig. (S20). Comparison of Antarctic CO_2, CH_4, and temperature records in several analyses of Antarctic ice core data.

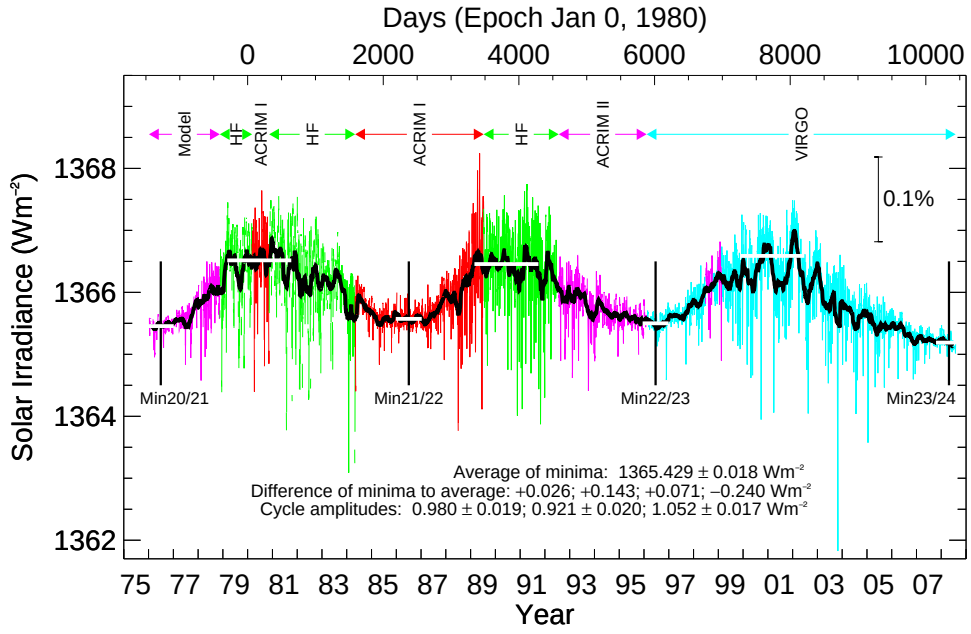

Fig. (S21). Solar irradiance from composite of several satellite-measured time series based on Frohlich and Lean [S44].

18. CLIMATE VARIABILITY, CLIMATE MODELS, AND UNCERTAINTIES

Climate exhibits great variability, forced and unforced, which increases with increasing time scale [2, 90, 91]. Increasing abilities to understand the nature of this natural variability and improving modeling abilities [S42] do not diminish the complications posed by chaotic variability for interpretation of ongoing global change.

Expectation that global temperature will continue to rise on decadal time scales is based on a combination of climate models and observations that support the inference that the planet has a positive energy imbalance [5, 8, 96]. If the planet is out of energy balance by +0.5-1 W/m^2, climate models show that global cooling on decadal time scales is unlikely [96], although one model forecast [95] suggests that the Atlantic overturning circulation could weaken in the next decade, causing a regional cooling that offsets global warming for about a decade.

The critical datum for determining the certainty of continued global warming on decadal time scales is the planet's energy imbalance. Improved evaluations of ocean heat storage in the upper 700 m of the ocean [97] yield ~0.5 x 10^{22} J/yr averaged over the past three decades, which is ~0.3 W/m^2 over the full globe. Our model has comparable heat storage in the ocean beneath 700 m, but limited observational analyses for the deep ocean [S43] report negligible heat storage.

If our modeled current planetary energy imbalance of 0.5-1 W/m^2 is larger than actual heat storage, the likely explanations are either: (1) the climate model sensitivity of 3°C for doubled CO_2 is too high, or (2) the assumed net climate forcing is too large. Our paleoclimate analyses strongly support the modeled climate sensitivity, although a sensitivity as small as 2.5 W/m^2 for doubled CO_2 could probably be reconciled with the paleoclimate data. The net climate forcing is more uncertain. Our model [8] assumes that recent increase of aerosol direct and indirect (cloud) forcings from developing country emissions are offset by decreases in developed countries.

These uncertainties emphasize the need for more complete and accurate measurements of ocean heat storage, as well as precise global observations of aerosols including their effects on clouds. The first satellite observations of aerosols and clouds with the needed accuracy are planned to begin in 2009 [98]. Until accurate observations of the planetary energy imbalance and global climate forcing are available, and found to be consistent with modeled climate sensitivity, uncertainties in decadal climate projections will remain substantial.

The sun is another source of uncertainty about climate forcings. At present the sun is inactive, at a minimum of the normal ~11 year solar cycle, with a measureable effect on the amount of solar energy received by Earth (Fig. **S21**). The amplitude of solar cycle variations is about 1 W/m^2 at the Earth's distance from the sun, a bit less than 0.1% of the ~1365 W/m^2 of energy passing through an area oriented perpendicular to the Earth-sun direction.

Climate forcing due to change from solar minimum to solar maximum is about ¼ W/m^2, because the Earth absorbs ~235 W/m^2 of solar energy, averaged over the Earth's surface. If equilibrium climate sensitivity is 3°C for doubled CO_2 (¾°C per W/m^2), the expected equilibrium response to this solar forcing is ~0.2°C. However, because of the ocean's thermal inertia less than half of the equilibrium response would be expected for a cyclic forcing with ~11 year period. Thus the expected global-mean transient response to the solar cycle is less than or approximately 0.1°C.

It is conceivable that the solar variability is somehow amplified, e.g., the large solar variability at ultraviolet wavelengths can affect ozone. Indeed, empirical data on ozone change with the solar cycle and climate model studies indicate that induced ozone changes amplify the direct solar forcing, but amplification of the solar effect is by one-third or less [S45, S46].

Other mechanisms amplifying the solar forcing have been hypothesized, such as induced changes of atmospheric condensation nuclei and thus changes of cloud cover. However, if such mechanisms were effective, then an 11-year signal should appear in temperature observations (Fig. **7**). In fact a very weak solar signal in global temperature has been found by many investigators, but only of the magnitude (~0.1°C or less) expected due to the direct solar forcing.

The possibility remains of solar variability on longer time scales. If the sun were to remain 'stuck' at the present solar minimum (Fig. **S21**) it would be a decrease from the mean irradiance of recent decades by ~0.1%, thus a climate forcing of about -0.2 W/m^2.

The current rate of atmospheric CO_2 increase is ~2 ppm/year, thus an annual increase of climate forcing of about +0.03 W/m^2 per year. Therefore, if solar irradiance stays at its recent minimum value, the climate forcing would be offset by just seven years of CO_2 increase. Human-made GHG climate forcing is now increasing at a rate that overwhelms variability of natural climate forcings.

Climate models are another source of uncertainty in climate projections. Our present paper and our estimated target CO_2 level do not rely on climate models, but rather are based on empirical evidence from past and ongoing climate change. However, the limited capability of models to simulate climate dynamics and interactions among climate system components makes it difficult to estimate the speed at which climate effects will occur and the degree to which human-induced effects will be masked by natural climate variability.

The recent rapid decline of Arctic ice [S47-S49] is a case in point, as it has been shown that model improvements of multiple physical processes will be needed for reliable simulation. The modeling task is made all the more difficult by likely connections of Arctic change with the stratosphere [S50] and with the global atmosphere and ocean [S51].

REFERENCES

[S1] Hewitt C, Mitchell J. Radiative forcing and response of a GCM to ice age boundary conditions: cloud feedback and climate sensitivity. Clim Dyn 1997; 13: 821-34.

[S2] Chylek P, Lohmann U. Aerosol radiative forcing and climate sensitivity deduced from the Last Glacial Maximum to Holocene transition. Geophys Res Lett 2008; 15: L04804, 1-5.

[S3] Schmidt GA, Ruedy R, Hansen JE, *et al.* Present day atmospheric simulations using GISS ModelE: Comparison to in-situ, satellite and reanalysis data. J Clim 2006; 19: 153-92.

[S4] Ingersoll AP. The runaway greenhouse: a history of water on Venus. J Atmos Sci 1969; 26, 1191-98.

[S5] Hoffman PF, Schrag DP. The snowball Earth hypothesis: testing the limits of global change. Terra Nova 2002; 14: 129-55.

[S6] Chandler MA, Sohl LE. Climate forcings and the initiation of low-latitude ice sheets during the Neoproterozoic Varanger glacial interval. J Geophys Res 2000; 105: 20737-56.

[S7] Wunsch C. The spectral description of climate change including the 100 ky energy. Clim Dyn 2003; 20: 353-63.

[S8] Jouzel J, Masson-Delmotte V, Cattani O, *et al.* Orbital and millennial Antarctic climate variability over the past 800,000 Years. Science 2007; 317: 793-6.

[S9] Medina-Elizade, M, Lea DW. The mid-Pleistocene transition in the Tropical Pacific. Science 2005; 310: 1009-12.

[S10] Hansen J, Sato M, Ruedy R, Lo K, Lea DW, Medina-Elizade M. Global temperature change. Proc Natl Acad Sci 2006; 103: 14288-93.

[S11] Lea DW, Pak DK, Spero HJ. Climate impact of late Quaternary equatorial Pacific sea surface temperature variations. Science 2000; 289: 1719-24.

[S12] Lea DW, Pak DK, Belanger CL, Spero HJ, Hall MA, Shackleton NJ. Paleoclimate history of Galapagos surface waters over the last 135,000 yr. Q Sci Rev 2006; 25: 1152-67.

[S13] Saraswat R., Nigam R., Weldeab S., Mackensen A, Naidu PD. A first look at past sea surface temperatures in the equatorial Indian Ocean from Mg/Ca in foraminifera. Geophys Res Lett 2005; 32: L24605.

[S14] Russell GL, Miller JR, Rind D. A coupled atmosphere-ocean model for transient climate change studies. Atmos-Ocean 1995; 33: 683-730.

[S15] Lisiecki LE, Raymo ME. A Pliocene-Pleistocene stack of 57 globally distributed benthic $\delta^{18}O$ records. Paleoceanography 2005; 20: PAI 003.

[S16] Bintanja R, van de Wal RSW, Oeriemans J. Modelled atmospheric temperatures and global sea levels over the past million years. Nature 2005; 437: 125-8.

[S17] Blakey R. Global paleogeographic views of Earth history – Late Precambrian to Recent 2008; http://jan.ucc.nau.edu/~rcb7/globaltext2.html

[S18] Royer DL, Berner RA, Beerling DJ. Phanerozoic atmospheric CO_2 change: Evaluating geochemical and paleobiological approaches. Earth-Science Rev 2001; 54: 349-92.

[S19] Fletcher BJ, Brentnall SJ, Anderson CW, Berner RA, Beerling DJ. Atmospheric carbon dioxide linked with Mesozoic and early Cenozoic climate change. Nature Geosci 2008; 1: 43-8.

[S20] Kurschner WM, Zlatko K, Dilcher DL. The impact of Miocene atmospheric carbon dioxide fluctuations on climate and the evolution of terrestrial ecosystems. Proc Natl Acad Sci 2008; 105: 449-53.

[S21] Cerling TE. Carbon dioxide in the atmosphere: Evidence from Cenozoic and Mesozoic paleosols. Am J Sci 1991; 291: 377-400.

[S22] Gray JE, Holroyd GH, Van der Lee FM, Bahrami AR, Sijmons PC, Woodward FI, Schuch W, Hetherington AM. The HIC signalling pathway links CO_2 perception to stomatal development. Nature 2000; 408: 713-16.

[S23] Woodward FI. Stomatal numbers are sensitive to increases in CO_2 from pre-industrial levels. Nature 1987; 327: 617-8.

[S24] Royer DL. Stomatal density and stomatal index as indicators of paleoatmospheric CO_2 concentration. Rev Palaeobot Palynol 2001; 114: 1-28.

[S25] Woodward FI, Bazzaz FA. The responses of stomatal density to CO_2 partial pressure. J Expert Bot 1988; 39: 1771-81.

[S26] Popp BN, Takigiku R, Hayes JM, Louda JW, Baker EW. The post-Paleozoic chronology and mechanism of 13C depletion in primary marine organic matter. Amer J Sci 1989; 289: 436-54.

[S27] Pagani M. The alkenone-CO_2 proxy and ancient atmospheric CO_2, In Understanding Climate Change: Proxies, Chronology, and Ocean-Atmosphere Interactions. Gröcke DR, Kucera M, Eds. Philos Trans Ro Soc Lond Series A 2002; 360: 609-32.

[S28] Spivack AJ, You C-F, Smith HJ. Foraminiferal boron isotope ratios as a proxy for surface ocean pH over the past 21 Myr. Nature 1993; 363: 149-51.

[S29] Blamart D, Rollion-Bard C, Meibom A, Cuif JP, Juillet-Leclerc A, Dauphin Y. Geochem Geophys Geosyst 2007; 8, 12: Q12001.

[S30] Lemarchand D, Gaillardet J, Lewin É, Allègre CJ. The influence of rivers on marine boron isotopes and implications for reconstructing past pH. Nature 2000; 4008:951-4.

[S31] Pagani M, Lemarchand D. Spivack A, Gaillarde J. A critical evaluation of the boron isotope-pH proxy: The accuracy of ancient ocean pH estimates. Geochimica et Cosmochimica Acta 2005; 69: 953-61.

[S32] Marland G, Boden TA, Andres RJ. Global, regional, and national fossil fuel CO_2 emissions. In trends: A compendium of data on global change. Carbon dioxide information analysis center, Oak Ridge National Laboratory, U.S. Department of Energy, Oak Ridge, Tenn., USA 2007; on-line at http://cdiac.esd.ornl.gov/trends/emis/meth_reg.htm

[S33] British Petroleum. Statistical Review of World Energy 2007 2007; on-line at http://www.bp.com/productlanding.do?categoryId=6848&contentId=7033471

[S34] Intergovernmental Panel on Climate Change (IPCC), Climate Change 2001: Mitigation. Davidson O, Metz B, Eds. Cambridge Univ Press: New York, 2001; pp. 753.

[S35] World Energy Council, Survey of Energy Resources; http://www.worldenergy.org/publications/survey_of_energy_resources_2007/default.asp 2007

[S36] Keeling CD, Whorf TP. Trends: A Compendium on Global Change; Carbon Dioxide Information Analysis Center, Oak Ridge Nat. Lab., US. DOE: Oak Ridge, TN 2005.

[S37] Intergovernmental Panel on Climate Change (IPCC), Land Use, Land-Use Change, and Forestry. Watson RT, Noble IR, Bolin B, Ravindranath NH, Verardo DJ, Dokken DJ, Eds. Cambridge Univ Press: Cambridge, UK 2000; pp. 377.

[S38] Lüthi D, Le Floch M, Stocker TF, Bereiter B, Blunier T, Barnola J-M, Siegenthaler U, Raynaud D, Jouzel J. Unexpected low levels of CO_2 concentration between 650 and 750 kyr BP. Nature 2008; (in press).

[S39] Loulergue L, Schilt A, Spahni R, Masson-Delmotte V, Blunier T, Lemieux B, Barnola J-M, Raynaud D, Stocker TF, Chappellaz J. Orbital and millennial-scale features of atmospheric CH_4 over the last 800,000 years. Nature 2008; (in press).

[S40] Parrenin F, Dreyfus G, Durand G, *et al.* 1-D-ice flow modelling at EPICA Dome C and Dome Fuji, East Antarctica. Clim Past 2007; 3: 243-59.

[S41] Dreyfus G, Parrenin F, Lemieux-Dudon B, *et al.* Anomalous flow below 2700 m in the EPICA Dome C ice core detected using $\delta^{18}O$ of atmospheric oxygen measurements. Clim Past 2007; 3: 341-53.

[S42] Sempf M, Dethloff K, Handorf D, Kurgansky MV. Toward understanding the dynamical origin of atmospheric regime behavior in a baroclinic model. J Atmos Sci 2007; 64: 887-904.

[S43] Levitus S, Anatov JI, Boyer TP. Warming of the world ocean, 1955-2003. Geophys Res Lett 2005; 32: L02604; doi:10.1029/2004GL021592.

[S44] Frohlich C, Lean J. 1998; (http://www.pmodwrc.ch/pmod.php?topic=tsi/composite/SolarConstant)

[S45] Hansen J, Sato M, Ruedy R. Radiative forcing and climate response. J Geophys Res 1997; 102: 6831-64.
[S46] Shindell D, Schmidt GA, Miller RL, Rind D. Northern Hemisphere winter climate response to greenhouse gas, volcanic, ozone, and climate. J Geophys Res 2001; 106: 7193-210.
[S47] Johannessen OM, Bengtsson L, Miles MW, *et al* Arctic climate change: observed and modeled temperature and sea-ice variability. Tellus 2004; 56A: 328-41.
[S48] Dorn W, Dethloff K, Rinke A, Kurgansky M. The recent decline of the Arctic summer sea-ice cover in the context of internal climate variability. Open Atmos Sci 2008; 2: 91-100.
[S49] Dorn W, Dethloff K, Rinke A, Frickenhaus S, Gerdes R, Karcher M, Kauker F. Sensitivities and uncertainties in a coupled regional atmosphere-ocean-ice model with respect to the simulation of Arctic sea ice. J Geophys Res 2007; 112: D10118; doi:10.1029/2006JD007814.
[S50] Brand S, Dethloff K, Handorf D. Tropospheric circulation sensitivity to an interactive stratospheric ozone. Geophys Res Lett 2008; 35: L05809; doi:10.1029/2007GL032312.
[S51] Dethloff K, Rinke A, Benkel A, *et al*. A dynamical link between the Arctic and the global climate system. Geophys Res Lett 2006; 33: L03703; doi:10.1029/2005GL025245.